Sediment phosphorus speciation and mobility under dynamic redox conditions

Chris T. Parsons[*1], *Fereidoun Rezanezhad*[1], *David W. O'Connell*[1,2], *Philippe Van Cappellen*[1]

[1]Ecohydrology Research Group and The Wate r Institute, University of Waterloo, 200 University Avenue West, Waterloo, Ontario, Canada.

[2]Department of Civil, Structural and Environmental Engineering, Trinity College Dublin, College Green, Museum Building, Dublin 2, Ireland.

[*]Corresponding author: Chris.Parsons@uwaterloo.ca

KEYWORDS: phosphorus, eutrophication, internal loading, redox cycling, bioturbation

ABSTRACT

Anthropogenic nutrient enrichment has caused phosphorus (P) accumulation in many freshwater sediments, raising concerns that internal loading from legacy P may delay the recovery of aquatic ecosystems suffering from eutrophication. Benthic recycling of P strongly depends on the redox regime within surficial sediment. In many shallow environments, redox conditions tend to be highly dynamic as a result of, among others, bioturbation by macrofauna, root activity,

sediment resuspension and seasonal variations in bottom water oxygen (O_2) concentrations. To gain insight into the mobility and biogeochemistry of P under fluctuating redox conditions, a suspension of sediment from a hyper-eutrophic freshwater marsh was exposed to alternating 7-day periods of purging with air and nitrogen gas (N_2), for a total duration of 74 days in a bioreactor system. We present comprehensive data time series of bulk aqueous and solid phase chemistry, solid phase phosphorus speciation and hydrolytic enzyme activities demonstrating the mass balanced redistribution of P in sediment during redox cycling. Aqueous phosphate concentrations remained low (~2.5 μM) under oxic conditions, due to sorption to Iron(III)-oxyhydroxides. During anoxic periods, once nitrate was depleted, the reductive dissolution of Iron(III)-oxyhydroxides released P. However, only 4.5% of the released P accumulated in solution while the rest was redistributed between the $MgCl_2$ and $NaHCO_3$ extractable fractions of the solid phase. Thus, under the short redox fluctuations imposed in the experiments, P remobilization to the aqueous phase remained relatively limited. Orthophosphate predominated at all times during the experiment in both the solid and aqueous phase. Combined P monoesters and diesters accounted for between 9 and 16% of sediment particulate P. Phosphatase activities up to 2.4 mmol h^{-1} kg^{-1} indicated the potential for rapid mineralization of organic-P (P_o), in particular during periods of aeration when the activity of phosphomonoesterases was 37% higher than under N_2 sparging. The results emphasize that the magnitude and timing of internal P loading during periods of anoxia are dependent on both P redistribution within sediments and bottom water nitrate concentrations.

Keywords:

^{31}P NMR, sequential extractions, coupled biogeochemical cycling, phosphorus, iron, sulfur, redox oscillation, redox fluctuation, bioreactor, internal loading

INTRODUCTION

It is widely recognized that accelerated eutrophication of freshwater aquatic environments is caused primarily by anthropogenic increases to dissolved phosphorus (P) concentrations in surface water (Smith and Schindler, 2009). Rapid cultural eutrophication of oligo or mesotrophic lacustrine and palustrine systems is often attributed to increased external P loadings originating in agricultural run-off or waste water treatment plant (WWTP) effluent. The resultant excessive algal growth negatively impacts aquatic ecosystems and economic activity (Pretty et al., 2003), as well as increasing the risk of infectious diseases (Chun et al., 2013). Strategies to mitigate eutrophication have aimed to reduce point source and diffuse external phosphorus loadings by instituting agricultural best management practices in the surrounding watershed (McLaughlin and Pike, 2014; Sharpley et al., 1994), limiting P inputs to domestic waste water (Corazza and Tironi, 2011) and upgrading WWTPs (Mallin et al., 2005). However, internal loading of P, from sediments to surface water, remains poorly quantified in many systems, and is often the largest source of error in hydrodynamic and ecological phosphorus models (Kim et al., 2013). Early diagenesis and mineralogical removal of labile autochthonous organic phosphorus (P_o) from solution is a complex process and is poorly understood in highly dynamic systems despite exerting a strong influence on the magnitude and timing of internal P loading. This is

59 particularly true in shallow lakes and wetlands due to the high sediment surface area to water
60 column depth ratio (Søndergaard et al., 2003).

61 As policy and infrastructure improvements continue in order to mitigate external P inputs to
62 aquatic systems, the relative importance of internal P loads from legacy P in sediments to overall
63 P budgets in eutrophic systems is likely to increase (Reddy et al., 2011).
64 It has been widely demonstrated through laboratory and field investigations, particularly in
65 seasonally anoxic lakes, that sustained anoxic conditions induced by water column stratification,
66 typically result in greater P mobility, and correspondingly higher water column P concentrations
67 (D. Krom and A. Berner, 1981; Einsele, 1936; Hongve, 1997; Katsev et al., 2006; Mortimer,
68 1941, 1971; Penn et al., 2000). The microbially mediated reductive dissolution of iron(III)
69 oxyhydroxides or iron(III) phosphate during sustained periods of anoxia at the sediment water
70 interface (SWI) has long been considered the main mechanism responsible for P release under
71 anoxic conditions e.g. (Bonneville et al., 2004; Hyacinthe and Van Cappellen, 2004).
72 More recently, considerable microbial polyphosphate accumulation and release in response to
73 alternating oxic-anoxic conditions at the SWI in lacustrine environments has also been shown to
74 occur (Gächter et al., 1988; Gächter and Meyer, 1993; Hupfer et al., 2007; Sannigrahi and Ingall,
75 2005). In some cases this accumulation of polyphosphate by the microbial community may
76 account for 10% of total phosphorus (Hupfer et al., 2007)
77 However, redox conditions in shallow, heavily bioturbated sediments are more spatially and
78 temporally variable than in seasonally anoxic lakes (Aller, 1994; Gorham and Boyce, 1989)
79 resulting in short term redox oscillations even with continuous oxia at the SWI.
80 Additionally, the coupled biogeochemical cycles of other redox sensitive elements such as sulfur
81 and carbon have been shown to play important and complex roles in phosphorus mobility

(Gächter and Müller, 2003; Joshi et al., 2015; O'Connell et al., 2015). For example, high bottom water sulfate concentrations have been shown to increase aqueous P in sediments by decreasing the permanent mineralogical removal of P within vivianite [$Fe_3(PO_4)_{2(s)}$] and by decreasing the abundance of iron(III) oxyhydroxides near to the SWI (Caraco et al., 1989). This is due to the scavenging of iron during the formation of iron sulfide minerals within sediment during diagenesis (Gächter and Müller, 2003). Carbon cycling also exerts considerable control over phosphorus mobility within sediment. The stoichiometry of freshly deposited organic matter (OM) in eutrophic water bodies approaches that of primary production i.e. ~C_{106}:N_{16}:P (Berner, 1977). Appreciable P may therefore be released to the aqueous phase when organic carbon is mineralized during microbial respiration of oxygen, nitrate, ferric iron or sulfate. In addition to driving N, Fe and S cycling, mineralization of organic carbon and concomitant P release has, in some places, been shown to be the primary mechanism controlling phosphorus mobility at the SWI (Joshi et al., 2015).

Core incubations and in-situ flux chambers frequently examine the effects of anoxia on P mobility from sediments but the effects of repetitive redox oscillations are rarely investigated in a controlled setting (Frohne et al., 2011; Matisoff et al., 2016; Nürnberg, 1988; Thompson et al., 2006). Consequently, the cumulative and reversible effects of oxic-anoxic cycling, on P distribution, speciation and mobility within sediments is poorly understood.

The aim of this study is to elucidate the microbial and geochemical mechanisms of in sediment phosphorus cycling and release associated with commonly occurring short redox fluctuations (days) in surficial sediments in shallow eutrophic environments. Particularly, we aimed to: 1) Quantify the redistribution of P between aqueous and mineral sediment pools during fluctuating redox conditions 2) Determine if the activity of hydrolytic phosphatase enzymes acting on P_o

were influenced by redox conditions, 3) Assess if the proportions of orthophosphate, P_o, and polyphosphate varied systematically with redox conditions and 4) Ascertain if P mobilization/immobilization mechanisms were reversible or cumulative.

We conducted controlled bioreactor experiments using sediment suspensions, designed to reproduce cyclic redox conditions analogous to those occurring in nature (Aller, .1994, 2004). A combination of aqueous chemistry, sediment sequential extractions (Ruttenberg, 1992), ^{31}P NMR spectroscopy (Cade-Menun, 2005) and extra-cellular enzyme assays (Deng et al., 2013) were used to produce a comprehensive dataset describing bulk chemistry, microbial and mineralogical controls on P mobility and speciation during redox oscillations.

METHODS

Field site and sampling

Surface sediment (0-12 cm), sediment cores (34 cm long, 10 cm diameter), overlying water and green filamentous algae (GFA) were collected on September 5, 2013 from West Pond in Cootes Paradise Marsh (43.26979N, 79.92899W) following established guidelines (U.S. EPA, 9/99). Cootes Paradise is a hyper-eutrophic, coastal freshwater marsh, which drains into Lake Ontario via Hamilton Harbour (see Figure 1A-1C). The marsh system suffered severe degradation due to rapid urbanization, population growth and nutrient loadings in the 20th century (Chow-Fraser et al., 1998). West Pond in particular received extremely high external P loads from the Dundas WWTP for several decades prior to the installation of sand filters in 1987 (Painter et al., 1991). The addition of sand filters, and other improvements, decreased P loadings from the WWTP from 45 kg P day^{-1} in the early 1970's (Semkin et al., 1976) to 4.5 kg P day^{-1} in the 1980s (Chow-Fraser et al., 1998) and 2.59 kg P day^{-1} in 2011 (Routledge, 2012). However, high

external P loads resulted in accumulation of legacy P in West Pond sediments with total phosphorus concentrations reaching 200 μmol g^{-1} by the 1980's (Theysmeyer et al., 1999). Consequently, dredging was conducted in 1999 in an attempt to remediate the areas most affected by growth of green filamentous algae (Bowman and Theysmeyer, 2014)

Despite these restoration efforts and decreases to the external P load, pervasive growth of GFA during the summer persists in parts of Cootes Paradise (Figure 1A). Cyanobacteria are not commonly observed at this location, potentially due to the high N:P ratios often associated with WWTP which utilize tertiary P removal treatment (Conley et al., 2009; Stumm and Morgan, 1996).

Sediment characterization

Sediment cores were sliced every 3 cm, homogenized and characterized with bulk sediment samples prior to bioreactor experiments. Organic carbon and carbonate depth profiles were determined by thermo-gravimetric analysis (TGA-Q500, TA Instruments Q500) (Pallasser et al., 2013). Water content and bulk density (ρ_b) of the sliced sediment core were determined gravimetrically after oven drying (Gardner, 1986). Identification and quantification of crystalline mineralogy was determined by powder X-ray diffraction (XRD) (Empyrean Diffractometer and Highscore Plus software Ver. 3.0e PANalytical). The density of benthic macro-invertebrates was also quantified after sieving two additional 7.5 cm diameter, 18 cm deep cores through 500 µm mesh.

Bioreactor experiment and redox oscillation procedure

An initial, concentrated, sediment suspension of approximately 500 g L^{-1} (dry weight equivalent) was prepared from freshly sampled sediment (0-12 cm) and filtered overlying water (< 0.45 μm).

149 Surface water was used, rather than distilled water, to provide background ionic strength and
150 avoid osmotic shock to the microbial community. The concentrated suspension was stirred
151 vigorously for 5 minutes then passed through a < 500 μm stainless steel sieve to remove larger
152 solid organic material and macro-invertebrates. This procedure was repeated until a
153 homogeneous suspension was achieved. The dry weight was then re-determined, and the sieved
154 solution was diluted with filtered surface water to a final concentration of 247 ± 2 g L^{-1}. The
155 resulting suspension was transferred to a bioreactor system (Applikon Biotechnology) after
156 Thompson et al (2006) and Parsons et al (2013). In addition to affording precise temperature
157 control and continuous logging of temperature, redox potential (E_h) and pH, the system offers
158 significant advancements over previous designs (Thompson 2006, Guo 2007, Parsons 2013). The
159 E_h, pH and dissolved oxygen (DO) were measured using a combined autoclavable Mettler
160 Toledo InPro 3253i/SG open-junction electrode and an AppliSens Low drift polarographic
161 sensor. The InPro electrode system, using a common reference electrode, was chosen to help
162 avoid potential interference between two electrodes in close proximity. A multi parameter
163 transmitter was used to display current pH, E_h and temperature, to automatically temperature
164 correct pH values and to adjust measured E_h to the standard hydrogen electrode (SHE). DO was
165 calibrated using 100% saturation in air (approximately 0.2905 atm) and 0% saturation in N_2 at
166 constant sparging of 30 ml min^{-1}

167 The suspension was stirred continuously and sparged with 30 mL min^{-1} air for 11 days to
168 equilibrate prior to the redox oscillation procedure. During the 11-day oxic equilibration period,
169 CO_2 emissions were monitored in the reactor exhaust gas using an IR sensor (Applikon
170 Biotechnology).

Subsequently, redox potential (E_h) variation was induced by the modulation of sparging gases (30 ml min^{-1}) between N_2:CO_2 and O_2:N_2:CO_2. The suspension was subjected to five cycles of anoxia (7 days) and oxia (7 days) at constant temperature (25^oC) in the dark, while recording E_h, pH, DO and temperature data. The suspension was sampled on days 1, 3, 5 and 7 of each half-cycle. To separate solid and aqueous components from the sediment suspension, syringe extracted samples (15 ml) were centrifuged at 5000 rpm for 20 minutes and the supernatant filtered through 0.45 μm polypropylene membrane filters prior to all aqueous analysis. For samples taken during anoxic half cycles, centrifugation, filtering and subsampling were performed in an anoxic glove box (N_2:H_2 97:3%, O_2 < 1 ppmv). Time periods were chosen to be representative of short temporal fluctuations to redox conditions experienced by surficial sediments (Aller, 1994; Nikolausz et al., 2008; Parsons et al., 2013). Similarly, the temperature and dark conditions were chosen to reflect those measured in surficial sediment during summer months at the field site. Summer conditions were chosen as this is when maximum bioturbation, microbial activity and OM input are expected within the sediment. Similar, long-running batch reactor experiments using soil or sediment have previously experienced a slowdown of metabolic processes due to depletion of labile organic carbon (Parsons et al., 2013). Therefore, gaseous carbon and nitrogen losses from the reactor were balanced by the addition of 3 g of freeze dried, ground, GFA to the suspension at the onset of each anoxic cycle. The amount of algae added was determined based on CO_2 production from the reactor during the initial 11 day oxic period.

Aqueous phase methods

All reagents used were of analytical grade from Fluka, Sigma-Aldrich or Merck unless stated otherwise and were prepared with 18.2 MΩ cm^{-1} water (Millipore). Total dissolved Na (70), K(100), Ca(20), Mg(0.5), Mn(1), Fe(3), Al(100), P (2), Si (15) and S (15) concentrations (MDL

194 in μg L^{-1}, in brackets) were determined by ICP-OES (Thermo Scientific iCAP 6300) after
195 filtration (< 0.45 μm) and acidification with HNO_3 to < pH 2. Matrix-matched standards were
196 used for all calibrations and NIST validated multi-elemental solutions were used as controls.
197 SRP concentrations were determined by the molybdenum blue/ascorbic acid method on a LaChat
198 QuickChem 8500 flow injection analyzer system (*4500-P E: Phosphorus by Ascorbic Acid*,
199 1992; Murphy and Riley, 1962) (MDL = 1.2 μg P L^{-1}). DOC was determined using a Shimadzu
200 TOC-LCPH/CPN analyzer (Shimadzu) following HCl addition (< pH 2) to degas dissolved
201 inorganic carbon (DIC) (MDL 71 μg C L^{-1}).
202 Chloride, nitrate, nitrite and sulfate concentrations were measured by ion chromatography using
203 a Dionex ICS 5000 equipped with a capillary IonPac® AS18 column. Aqueous sulfide was
204 stabilized with 20 μL 1% zinc acetate per mL (Pomeroy, 1954) after filtering and determined by
205 the Cline method (Cline, 1969) (MDL 0.5 µM). $Fe^{2+}_{(aq)}$ was determined by the ferrozine method
206 immediately after filtering (Stookey, 1970; Viollier et al., 2000) (MDL 3.8 μM). All aqueous
207 analyses were conducted in triplicate. The precision and accuracy for all techniques was < 5
208 RSD% and ±10% with respect to certified reference materials (where commercially available).

209 **Solid phase methods: Phosphorus and Iron Speciation**

210 Phosphorus partitioning within the solid phase in the reactor experiment was evaluated over a
211 time series by both sequential extractions, using a modification (Baldwin, 1996) of the SEDEX
212 extraction scheme (Ruttenberg, 1992) and solution ^{31}P NMR spectroscopy (Cade-Menun, 2005).
213 The two approaches are complementary; ^{31}P NMR spectroscopy provides information on the
214 molecular speciation of phosphorus, while sequential extraction provides information on the
215 association of the P species with operationally defined solid phase fractions. Therefore the

combination of these two methods reveals redistribution of P within the solid phase over time during oxic-anoxic transitions.

The original SEDEX extraction scheme quantifies five different P reservoirs within sediment by consecutively solubilizing progressively more recalcitrant phases by using extracts of increasing severity. The reaction mechanisms associated with each extraction step are discussed in detail within Ruttenberg (1992). A modification of the SEDEX extraction scheme proposed by Baldwin (1996), used here, incorporates an additional 16 hour, 1M $NaHCO_3$ step (P_{Hum}) after the P_{Ex} step, to differentiate OM associated P which may otherwise be co-extracted during the P_{Fe} step. The pH of the $NaHCO_3$ extraction step was adjusted to 7.6 to minimize dissolution of carbonates prior to the P_{CFA} extraction step. A total of 15 samples between day 11 and 74 of the reactor experiment were analyzed in duplicate by sequential extraction. A summary of the full sequential extraction method used, including target phases, reactants, pH, temperature and reaction times is provided in Table 1.

Changes to iron speciation were also evaluated through a time series during the experiment. To account for surface-sorbed or freshly precipitated Fe, total Fe^{2+} production during anoxic half-cycles was estimated by a partial extraction (1 hour, 0.5N HCl) on sampled suspensions. Fe^{2+}/Fe^{3+} ratios were determined in extracts using a modification of the ferrozine method (Stookey, 1970; Viollier et al., 2000). Additionally, a thermodynamic model was implemented in PHREEQC (Parkhurst et al., 1999) to assess the saturation index (SI) of various minerals over time during the reactor experiment using measured pH, temperature, E_h and concentration data.

NaOH-EDTA Extraction and Solution ^{31}P NMR Spectroscopy

Molecular changes to P speciation were evaluated over a time series by solution ^{31}P NMR. Phosphorus was extracted directly from suspension samples (~2 g dry weight equivalent) prior to ^{31}P NMR analysis. The method used has been shown to allow quantitative analyses of P_o (monoester and diester), polyphosphates and orthophosphate (Amirbahman et al., 2013; Cade-Menun et al., 2006, p.; Cade-Menun and Preston, 1996; Reitzel et al., 2007; Turner et al., 2003b). Briefly, Samples were extracted in 25 mL of 0.25 M (NaOH) and Na_2EDTA (0.05 M) at ambient laboratory temperature (~22 ^{o}C) for 4 hours. Subsequently, the tubes were centrifuged (3500 rpm for 20 minutes), the supernatant extracted via syringe then neutralized with 2M HCl to a pH of 7 to avoid the breakdown of polyphosphates during freeze drying (Cade-Menun et al., 2006). This solution was then filtered to < 0.45 μm. Prior to freeze-drying 1 mL aliquots of each sample were diluted and analyzed by ICP-OES spectroscopy for Al, Ca, Fe, Mg, Mn and P. The remaining extracts were frozen at -80 ^{o}C and lyophilized for 48 hours. The lyophilized extracts were re-dissolved in 1.0 ml D_2O, 0.6 ml 10 M NaOH, and 0.6 ml of the NaOH-EDTA extractant solution and were allowed to stand for 10 min with occasional vortexing. Samples were centrifuged for 20 min at 3500 rpm, transferred to 10-mm NMR tubes, and stored at 4 °C before analysis within 12 hours.

Solution ^{31}P NMR spectra were obtained using a 600-MHz spectrometer equipped with a 10-mm broadband probe. The NMR parameters were: 90° pulse, 0.68-s acquisition time, 4.32-s pulse delay, 12 Hz spinning, 20 °C, 2200 to 2900 scans (3-4h) for 0-5cm sediment samples (Cade-Menun et al., 2010). Phosphorus compounds were identified by their chemical shifts related to an external orthophosphoric acid standard, with the orthophosphate peak in all spectra standardized to 6ppm. Peak areas were calculated by integration on spectra processed with 10 and 7-Hz line

broadening, using NUTS software (Acorn NMR, Livermore CA, 2000 edition). Peak assignments were grouped into compounds or groups of specific compound classes if direct identifications could not be made (Cade-Menun, 2005).

Extracellular enzyme assays

Rates of enzymatic hydrolysis of P_o were estimated through extracellular enzyme activities (EEA). Degradation rates for phosphomonoesters, phosphodiesters and pyrophosphate were determined fluorometrically through use of the MUF tagged substrates; MUF phosphate (MUP), Bis(MUF)phosphate (DiMUP, Chem-Impex International), and MUF pyrophosphate, (PYRO-P), Chem-Impex International) respectively. Additionally MUF β-D-glucopyranoside (MUGb) was used in order to compare phosphatase enzyme activity to the activity of β-glucosidase (cellulase) (Dunn et al., 2013). Enzyme activities were determined using a microplate reader (Flexstation3, Molecular Devices) using a modification of Deng et al (2013). Briefly, 1 g dry weight equivalent of suspension from the reactor was stirred with 100 mL of 100 mM HEPES buffer at pH 7.5 in a pyrex dish for 10 minutes at 280 rpm to allow for complete homogenization. Subsamples (100 μL) of the buffered soil suspension were removed during continuous mixing using a multi-channel pipette and placed into microplate wells, which were loaded into the microplate reader. Four replicate wells were filled per substrate. Plates were left to equilibrate at 30 ^{o}C for 5 minutes inside the reader before the automatic addition of 100 μL of substrate, resulting in a final substrate concentration of 667 μM. Each well was triturated thoroughly during addition of the substrate. Excitation fluorescence was set at 365 nm. Emission intensity at 450 nm was recorded at 5-minute intervals over a 6-hour period. The effect of fluorescence quenching was accounted for in each sample by preparing MUF calibration curves in the same soil suspension as used for the analysis. The limits of detection and quantification were

282 determined to be 1.1 µM and 3.3 µM MUF respectively, equivalent to 1.1 µM of phosphate for
283 the determination of phosphomonoesterase activities.

284 RESULTS & DISCUSSION

285 Sediment characterisation and evidence of bioturbation

286 Characterisation of sediment cores revealed physical and chemical solid phase homogeneity
287 within the top 10 cm, with a bulk density of ~1.3 g cm^{-3}, water content of ~50% (by weight), OM
288 of ~3% and a carbonate of ~25% (Figure 2B). Between 10 and 15 cm depth increases in bulk
289 density and decreases to the sediment water content, OM % and carbonate fraction occurred as
290 soft sediment transitioned to clay.

291 A benthic macroinvertebrate density of approximately 49,500 individuals per m^2 was
292 determined, consistent with previously reported values (Pelegri and Blackburn, 1995). The
293 community (Figure 2A) was dominated by aquatic earthworms (*Tubificidae 60%* and *Branchiura*
294 *sowerbyii 8%*) which typically feed and mix sediment within the top 5-10 cm (Fisher et al., 1980;
295 McCall and Fisher, 1980). Other groups identified included *Ceratopogonidae* (No see ums or
296 biting midges, 22%) including *Sphareomias*, *Probezzia* and *Bezzia, Chironomidae* (Midges, 6%)
297 including *Cryptochironomus* and *Tanypus, Nemotoda* (round worms, 4%) and a single *Hyalella*
298 *azteca* (scud <1%).

299 Bioturbating organisms, such as those identified, have previously been shown to alter
300 biogeochemical cycling within surface sediments (Hölker et al., 2015). Reported influences
301 include increased solute fluxes (Furukawa et al., 2001; Matisoff and Wang, 1998), mixing of
302 solid sediment (Fisher et al., 1980) and bioconveying of sediment particles (Lagauzère et al.,

2009). These processes have been shown to enhance sediment oxygen demand (McCall and Fisher, 1980; Pelegri and Blackburn, 1995), degradation of OM (Aller, 1994), rates of denitrification, transport of contaminants to surface water (Lagauzère et al., 2009), and temporal fluctuation of redox conditions (Aller, 1994). Efficient sediment mixing allows frequent re-oxidation of reduced sediments and therefore regeneration of terminal electron acceptors (TEAs) such as nitrate, ferric iron and sulfate, which often limit mineralisation of OM in sediments underlying hypereutrophic water bodies (Reddy and DeLaune, 2008). Electron donors in the form of fresh autochthonous necromass are also rapidly redistributed vertically within the zone of bioturbation. This environment should therefore support a metabolically diverse, abundant and highly active microbial community (DeAngelis et al., 2010).

Quantitative XRD analysis of the top 12 cm of sediment (Figure 2C) showed close agreement with the carbonate fraction determined by TGA (~25% by TGA vs 27% by XRD) indicating a calcite dominated, carbonate buffered system. The remaining mineral assemblage was dominated by quartz and clay minerals (Illite, 30% and Chamosite, 2%). No pyrite or vivianite was detected by XRD suggesting either their absence or presence in low abundance (<1%) with poorly crystalline structures.

Experimental redox oscillation: Aqueous chemistry

E_h within the bioreactor oscillated between +470 and -250 mV (Figure 3) consistent with E_h ranges of wetland sediments (Nikolausz et al., 2008). A slight pH oscillation was also present between ~7.4 during anoxic half-cycles (N_2 sparging) and ~7.7 during oxic-half cycles (N_2:O_2:CO_2 sparging), this variation, shown in Figure 3, is consistent with calcite/dolomite buffered sediment equilibrating with changing p_{CO2} caused by sparging gas composition and microbial respiration. After the 11-day equilibration, ionic strength of the aqueous phase in the

reactor suspension remained at ~0.025 +/- 0.004 M for the duration of the experiment. This range of E_h/pH conditions and ionic strength is consistent with the range measured within surficial sediment at the field site and transitions across the thermodynamically predicted stability boundaries for multiple redox couples e.g. MnO_2/Mn^{2+}, $NO_3^-/NO_2^-/NH_4^+$, $Fe(OH)_3/Fe^{2+}$, SO_4^{2-}/HS^-, during each 14 day redox cycle. The upper E_h values recorded during oxic cycles are significantly lower than predicted by the O_2/H_2O couple (820 mV @ pH 7) but are consistent with the O_2/H_2O_2 couple (300 mV @ pH 7) which is considered to control electrode measured E_h under oxic conditions (Stumm and Morgan, 1996).

Aqueous chemistry data, shown in Figure 3, demonstrate the consumption of TEAs in order of decreasing nominal energetic yield, coupled to the oxidation of labile OM. Upon physical removal and consumption of residual oxygen by aerobic respiration, nitrate concentration decreased in the solution. Decreases to nitrate concentration coincided with peaks of nitrite concentration within the first hour of oxygen removal, indicative of microbial denitrification. Subsequent increases to $Mn_{(aq)}$, $Fe^{2+}_{(aq)}$ and $HS^-_{(aq)}$ imply sequential reduction of MnO_2, $Fe(OH)_3$ and SO_4^{2-} as more energetically efficient electron acceptors were depleted. Mn (predicted as Mn^{2+} by the thermodynamic model) and Fe^{2+} were detected in solution earlier within each subsequent anoxic cycle, however the apparent order of reduction remained consistent across all five redox cycles (O_2, NO_3^-, NO_2^-, MnO_2, $Fe(OH)_3$, SO_4^{2-}). The consistent order and relative magnitude of reduction implies that the main biogeochemical functioning of the sediment suspension did not change dramatically between cycles during the experiment.

Although relatively low concentrations of Fe^{2+} (up to 71 μM) were measured in solution, 0.5 M HCl extractions revealed that significantly greater Fe^{2+} was produced during each anoxic cycle than was measured in the aqueous phase. Fe^{2+} generated by dissimilatory iron reduction has been

shown to sorb to mineral surfaces in sediment (Gehin et al., 2007; Klein et al., 2010; Liger et al., 1999) or precipitate as ferrous carbonate (Jensen et al., 2002), ferrous sulfide or other mixed ferrous/ferric phases (Rickard and Morse, 2005). The 0.5M HCl extractions targeted this sorbed or poorly crystalline freshly precipitated Fe^{2+}. During each anoxic cycle HCl extractable Fe^{2+} concentration increased by 50 to 70 μmol g^{-1}, equivalent to 12.31 to 17.29 mM of iron reduction within the reactor as a whole. Thus, only 0.63 +/- 0.4% of microbially reduced Fe^{2+} was measureable in solution. The aqueous phase of the reactor was shown to be supersaturated with respect to mackinawite (FeS), pyrite (FeS_2), vivianite ($Fe_3(PO_4)_2$:$8H_2O$) and siderite ($FeCO_3$) during anoxic half-cycles indicating thermodynamic favourability for precipitation of these minerals. The kinetic constraints on precipitation were not, however, considered. No significant cumulative change to extractable Fe^{2+}/Fe^{3+} occurred after five full reduction-oxidation cycles, indicating that solid phase Fe redox cycling was reversible, potentially due to rapid oxidation of solid Fe^{2+} in the presence of O_2 and carbonate (Caldeira et al., 2010).

DOC concentration also fluctuated systematically during oxic-anoxic cycles (Figure 3). Higher DOC concentrations were measured during anoxic conditions than oxic conditions. DOC may be replenished by both enzymatic hydrolysis of particulate organic matter (POM) (Vetter et al., 1998) and desorption of mineral associated OM (Grybos et al., 2009). The addition of algal matter at the beginning of anoxic cycles resulted in observable sharp peaks of DOC which was rapidly removed from solution, probably due to a combination of mineralization of labile DOC to HCO_3^- and sorption processes (Chorover and Amistadi, 2001; Grybos et al., 2009). The peak of DOC supplied by addition of algal matter represented labile DOC, which was readily mineralized in comparison to the residual DOC, which persisted in the system throughout the experiment. The differences in residual OM mobility between oxic and anoxic cycles were

372 unlikely due to oxide dissolution as differences to DOC concentration are observed prior to
373 increases in Mn and Fe concentration in solution. We therefore postulate that solubility changes
374 to humified DOC were driven by pH changes (Figure 3) between oxic and anoxic conditions
375 caused by changes in pCO_2 between oxic and anoxic conditions as previously shown by Grybos
376 et al in wetland sediments (Grybos et al., 2009).

377 Lowest aqueous phosphorus concentrations (~2.5 to 3 μM), shown in Figure 4, occurred during
378 oxic half cycles and increased dramatically during anoxic half cycles to a maximum
379 concentration of 50 to 60 μM per cycle, 88% of which occurred as SRP. The range of TDP
380 concentrations within the aqueous phase of the reactor suspension are similar to those reported in
381 situ at the field site by Mayer et al (2006). The timing of phosphorus release to the aqueous
382 phase corresponded well with increasing $Fe^{2+}_{(aq)}$ concentration. This is reflected in a strong
383 positive correlation between TDP and Fe concentrations ($n = 37$, $R^2 = 0.93$, $p < 0.0001$).
384 Increases to aqueous P concentration occurred only after depletion of residual O_2, NO_3^- and NO_2^-,
385 after increases to $Mn_{(aq)}$ and before increases to $HS^-_{(aq)}$. The timing of P release is suggestive of an
386 iron(III)-oxyhydroxide or ferric phosphate control on phosphorus mobility (Bonneville et al.,
387 2004; Hyacinthe and Van Cappellen, 2004) and indicates that complete nitrate depletion was
388 required prior to phosphorus release to the aqueous phase.
389 Full tabulated aqueous chemistry data for the experimental time series is provided as supporting
390 information.

391 **Sequential chemical extractions and solid phase P partitioning**

392 The sum of P concentrations from all sequential extraction reservoirs (61 ± 5 μmol g^{-1}) was
393 consistently within 10% of a total P extraction (57 ± 4 μmol g^{-1}) indicating acceptable analytical
394 precision from the sequential extraction procedure. Highest P concentrations were associated

395 with the P_{Hum} (~26% of TP) and P_{Fe} (~24%) fractions with lower P concentrations in the P_{Ex}
396 ~16%, P_{CFA} ~15%, P_{Detr} ~12% and P_{Res} ~7% fractions (Figure 4). The largest variations in P
397 concentration were observed for P_{Fe} and decreased in the order P_{Fe} (2.6) > P_{Hum} (1.5) > P_{Ex} (0.4) >
398 P_{Detr} (0.4) > P_{Resi} (0.35) > P_{CFA} (0.25), where the numbers in brackets are standard deviations
399 (μmol g^{-1}). High variability over time within the P_{Fe} and P_{Hum} fractions suggests that P was
400 exchanged to and from these fractions during redox oscillation whereas changes to the P_{Ex}, P_{Resi}
401 and P_{CFA} fractions were comparatively insignificant (Figure 4).
402 The P_{Fe} fraction was the only P pool in which concentration consistently decreased during anoxic
403 conditions and increased during oxic conditions (Figure 4). When a P mass balance (Figure 5)
404 was attempted to account for increases to aqueous phosphorus (P_{Aq}) from the iron bound (P_{Fe})
405 pool during anoxic periods it became evident that only approximately 4.5% of variability
406 observed in the P_{Fe} pool (total P_{Fe} variation of up to 4.5 μmol g^{-1} during anoxic periods) was
407 necessary to account for the changes to inter-cycle P_{Aq} concentrations (50 μM). The remainder of
408 P_{Fe} lost during anoxic cycles appears to be reversibly redistributed to the P_{Ex} (~30%) and P_{Hum}
409 (~65%) pools which generally increased during anoxic conditions and decreased during oxic
410 conditions (Figure 4).
411 According to Ruttenberg (1992) the P_{Ex} fraction corresponds to P mobilised via the formation of
412 $MgPO_4^-$ complexes and(or) mass action displacement by Cl^-. It is therefore considered that
413 $MgCl_2$ effectively extracts P loosely associated with mineral surfaces. However, Ruttenberg
414 (1992) also demonstrated that plankton were efficiently extracted by $MgCl_2$ as well as ~25% of P
415 associated with biogenic $CaCO_3$. Consequently, it is likely that P associated with microbial
416 biomass, $CaCO_3$, and other loosely sorbed P contributed to the P_{Ex} fraction. Slight increases to P_{Ex}
417 concentration during anoxic periods and corresponding decreases during oxic periods likely

418 reflect the combination of two processes 1) equilibration between P surface complexes and
419 aqueous P species due to fluctuating aqueous concentrations which were consistently higher
420 during anoxic periods (Olsen and Watanabe, 1957) and 2) pH driven sorption/desorption as pH
421 was consistently slightly higher during aerobic periods (Figure 3) favouring desorption from
422 mineral surfaces including illite which comprised 30% of the crystalline mineralogical fraction
423 (Figure 2C) (Manning, 1996).
424 The $NaHCO_3$ extraction step was originally added to the SEDEX method to target OM
425 associated P, which would otherwise be liberated during the P_{Fe} extraction step (Baldwin, 1996).
426 Baldwin noted a brown coloration in P_{Hum} extracts and that absorbance at 250 nm was positively
427 correlated with SRP. Absorbance at 254 nm has been shown to be indicative of aromatic OM,
428 commonly associated with humic substances (Weishaar et al., 2003). A light brown color was
429 also present in the $NaHCO_3$ extracts recovered during this experiment despite comparatively low
430 sediment OM content (Figure 2B). Absorbance spectra for these extracts were not determined.

431 Li et al (2015) have recently demonstrated that the SEDEX P_{Fe} extraction step co-extracted P
432 associated with fine iron oxide-OM complexes when a prior $NaHCO_3$ step was not incorporated.
433 However, Li et al (2015) also suggested that these complexes may be more recalcitrant than pure
434 minerals. Iron was present within the P_{Hum} extract at concentrations between 18 and 25 μmol g^{-1}
435 however, the original speciation of this iron is prior to extraction is unknown. Chemically similar
436 extractions used in soil sciences such as Hedley's extraction (0.5 M $NaHCO_3$, pH 8.5, 16 hours)
437 and the Olsen-P test (0.5M $NaHCO_3$, pH 8.5, 30 minutes) have been shown to extract Mg and Ca
438 phosphates as well as some organic P (Hedley et al., 1982; Olsen et al., 1954). Approximately
439 2/3 of P extracted within P_{Hum} was present as SRP suggesting that ~1/3 of this fraction may be P_o
440 species. The pH of the $NaHCO_3$ extract used here was adjusted to 7.6 to minimize the dissolution

441 of Mg and Ca phosphates prior to the P_{CFA} extraction. Despite this, 30 to 44 μmol g^{-1} of Ca was
442 extracted within the P_{Hum} fraction. The origin of the extracted Ca is, however, unknown and may
443 have been complexed with OM or part of labile Ca-phosphates. It is still expected that the
444 majority of Ca-phosphate minerals were quantified as part of the P_{CFA} or P_{Detri} extractions which
445 included ~500 to 700 and ~50 to 70 μmol Ca g^{-1} respectively.

446 Humic acids are known to compete with orthophosphate for surface binding sites on various
447 minerals including goethite (Sibanda and Young, 1986) and poorly ordered Fe-oxides in the
448 short term (Gerke, 1993). However, sorption of natural OM to freshly precipitated Fe oxides may
449 increase the long term sorption capacity of ferric oxides towards P by decreasing
450 recrystallization over time (Gerke, 1993) and through the formation of OM-Fe-P complexes
451 (Gerke, 1993). Although previous studies have provided evidence for ternary complexes between
452 ferric iron, OM and phosphate (Kizewski et al., 2010b) there is currently no direct spectroscopic
453 evidence for the existence of mixed OM-Fe(III)-phosphate complexes in natural waters.
454 Identification of such complexes in natural environments is inherently challenging due to the
455 complexity of natural geochemical matrices (Kizewski et al., 2010a). Recent studies have
456 however successfully investigated the structure of synthetic OM-Fe(III)-phosphate complexes
457 (Kizewski et al., 2010a) and similar OM-Fe(III)-arsenate complexes spectroscopically (Mikutta
458 and Kretzschmar, 2011; Sharma et al., 2010). These studies suggest that similar and perhaps
459 more complex heterogeneous ternary complexes are also likely to be present in natural
460 freshwater environments (Kizewski et al., 2010a). This suggestion is also supported by the
461 observation that more than 80% of soluble P in some natural waters is associated with high
462 molecular weight OM (Gerke, 2010). As spectroscopic characterization of the P associated with
463 the P_{Hum} fraction was not performed in this study, the P_{Hum} pool is considered to represent a

464 variety of OM associated P in addition to small amounts of P from labile Ca-phosphate minerals.
465 OM associated P extracted within this fraction is likely coordinated with ferric iron (18 to 25
466 μmol Fe g^{-1} coextracted), Ca (30 to 44 μmol Ca g^{-1} coextracted) or Al (0.8 to 1.5 μmol Al g^{-1}
467 coextracted). These metals may, in-turn, be associated with various mineral surfaces within the
468 sediment.

469 Sequential extraction data demonstrate that the P_{Hum} fraction is the dominant P fraction in all
470 samples analysed, which highlights the significance of this fraction. P mass balance also suggests
471 that reversible re-partitioning between this and the P_{Fe} fraction occurs during redox condition
472 changes. As the exact chemical nature of the P_{Hum} fraction is not known, interpretation of
473 concentration changes over time are challenging. Speculatively, increases to the P_{Hum} fraction
474 under anoxic conditions may be due to the release of occluded OM-metal-P complexes within
475 iron(III) oxyhydroxides during reductive dissolution or simply re-equilibration of solid phase
476 OM-metal-P complexes with increased aqueous P.

477 We consider that the majority of P extracted within the P_{Fe} fraction was co-precipitated with
478 iron(III)-oxyhydroxides which were reductively dissolved by dithionite during the extraction
479 (Ruttenberg, 1992). This interpretation is supported by the relatively high concentrations of iron
480 extracted within the P_{Fe} fraction (72 to 91 μmol Fe g^{-1}). Aqueous Fe^{2+} produced during this
481 extraction is subsequently chelated by citrate and therefore solubility of Fe and P is maintained.
482 The bicarbonate component functions as a pH buffer to ensure maximum preservation of apatite
483 and $CaCO_3$ bound P during this reaction step (Ruttenberg, 1992).
484 Neither the P_{CFA}, P_{Detri} nor P_{Resi} fractions varied systematically between oxic and anoxic
485 conditions, or changed consistently during the course of the experiment, suggesting their
486 comparative stability during short periods of redox fluctuation this is supported by calculated

487 saturation indices (SI) for hydroxyapatite, which remained between +0.86 and +6.24 for the
488 duration of the experiment.
489 The P contribution from individual algal additions (~1.5 μmol P g^{-1}) was relatively small
490 compared to total P in the reactor (61 μmol P g^{-1}) and within the margin of analytical error
491 associated with solid extractions. Additionally, no single fraction shows a clear increase over the
492 course of the experiment, therefore quantification of the redistribution of P added with algal
493 additions is not possible.
494 Full tabulated solid phase chemistry data for the experimental time series is provided as
495 supporting information.

496 **Fe:P ratios**

497 Sequential extraction data, shown in Figure 4, aqueous chemistry data shown in Figure 3, and the
498 correlation between aqueous Fe and P ($n = 37$, $R^2 = 0.93$, $p < 0.0001$) all suggest that P released
499 to solution under anoxic conditions originated in the P_{Fe} pool. Although the maximum molar
500 ratio for phosphate incorporation within ferric oxides has been shown to be 2:1 (Fe:P) (Thibault
501 et al., 2009), it has been suggested that much higher solid Fe:P of 15 (Jensen et al., 1992) to >20
502 (Phillips et al., 1994) maybe necessary to control phosphorus mobility under oxic conditions.
503 Results from bioreactor experiments suggest that phosphorus is retained in the solid phase under
504 oxic conditions at total Fe:P ratios of just 4.1:1, potentially due to the association of P with other
505 solid sedimentary pools, particularly P_{Hum}. Fe:P ratios below the stoichiometric limitation of 2:1,
506 measured in the aqueous phase (1.5 to 1.9), during anoxic conditions are therefore likely due to
507 the removal of Fe^{2+} from solution by secondary sorption and precipitation processes, subsequent
508 to reductive dissolution. Probable secondary Fe^{2+} removal processes include the formation of
509 amorphous FeS (SI of up to +2.27 for mackinawite) (Rickard and Morse, 2005) and sorption of

510 Fe^{2+} to clays (Gehin et al., 2007; Klein et al., 2010). This is supported by increases to Fe^{2+}/Fe^{3+}
511 ratios in the 0.5 M HCl extractable fraction during anoxic conditions. Frequent rapid reoxidation
512 of ferrous sulfide due to air sparging in the reactor experiment, and extensive bioturbation in-
513 situ, likely prevents formation of more recalcitrant and slow forming iron sulfide minerals such
514 as pyrite, despite strong thermodynamic favourability for pyrite formation (SI up to +13.13)
515 (Caldeira et al., 2010; Peiffer et al., 2015). This is consistent with the results of XRD analysis,
516 which did not identify pyrite (Figure 2C). A similar effect has been previously demonstrated in
517 lake sediments (Gächter and Müller, 2003).

518 **Hydrolytic enzyme activities**

519 The activities of model phosphomonoesterases, phosphodiesterases and pyrophosphatase were
520 found to be systematically higher under oxic conditions compared to anoxic conditions by 37%
521 ($p < 0.005$), 8% (not significant) and 24% ($p = 0.08$) respectively (Figure 6B).
522 Phosphomonoesterases were found to have the highest activities despite the inherent
523 overestimation of phosphodiesterase activities when using MUF tagged substrates (Sirová et al.,
524 2013). The opposite trend was observed for glycopyranoside, part of the cellulose degradation
525 pathway (Dunn et al., 2013), which showed consistently higher activity (69% $p = <0.05$) under
526 anoxic conditions (Figure 6B). The different trends exhibited by cellulose and phosphatase
527 enzymes, indicate that changes in activity were not universal but specific to enzyme function.
528 Phosphomonoesterase activities obtained in the current study (1.76 to 2.4 mmol h^{-1} kg^{-1}) are
529 similar to those previously reported in wetland sediments (Kang and Freeman, 1999) and suggest
530 the capacity for rapid hydrolysis of P_o species in necromass. Lowering of the water table in
531 wetlands has previously been shown to increase the activity of phosphatase enzymes and the
532 hydrolysis of P_o species (Song et al., 2007). However, water table fluctuation results in

concomitant changes to moisture content and redox conditions which prevents isolation of the causal variable in field investigations (Rezanezhad et al., 2014). Therefore, this is to the best of our knowledge, the first direct demonstration of phosphatase activity changes in response to changing redox conditions. We postulate that under anoxic conditions when phosphorus availability in the aqueous phase is high, production of extracellular phosphatase enzymes by the microbial community is down regulated. Conversely, when bioavailable phosphorus is removed from solution under oxic conditions, extracellular phosphatase production is up regulated in response. Adjustments to enzyme production in response to changes in phosphate availability must occur on short timescales (hours/days) for such trends to be observable during the bioreactor experiment. An inverse relationship between phosphatase activities and phosphate concentration, has previously been shown spatially in wetlands by Kang and Freeman (1999) but to our knowledge never temporally in sediments.

^{31}P NMR

Results from ^{31}P NMR analyses (Figure 6A) show that the majority of phosphorus was present in the solid phase as ortho-phosphate (84-91%) with 4-8% monoester P, 3-8% diester P and <1% phosphonates and polyphosphates with no clear trend in relative abundance emerging during the experiment. The NaOH-EDTA extraction resulted in a recovery of ~27% of TP, which is comparable to previous studies with carbonate buffered soils and sediments (Hansen et al., 2004; Turner et al., 2003a). Alpha and beta glycerophosphates are commonly identified in monoester spectral regions and have been demonstrated to be products of diesters degraded during analysis (Doolette et al., 2009; Jørgensen et al., 2015; Paraskova et al., 2015). As no glycerophosphates were identified in any of the analysed samples, recalculation of monoester/diester ratios was not performed. A higher mean monoester/diester ratio (2.31) was found in reduced samples than

556 oxidised samples (0.97) a statistically significant difference (p=0.04). This difference could
557 indicate that monoester P was either less efficiently extracted under oxic conditions due to
558 sorption to metal oxides or that monoesterase/diesterase activity decreased under anoxic
559 conditions, which is consistent with enzymatic activity assays (Figure 6B). Total P_o determined
560 by ^{31}P NMR varied between 9 and 16% over time compared to 5 to 11% in the P_{resi} from
561 sequential extractions, indicating that not all P_o was extracted in the P_{resi} fraction, which is
562 commonly referred to as the organic-P fraction. We postulate that the remaining ~5% of total
563 phosphorus, identified as P_o by ^{31}P NMR was extracted during previous steps in the sequential
564 extraction scheme, particularly $MgCl_2$, which has been shown to efficiently extract P associated
565 with microbial biomass (Ruttenberg, 1992) and $NaHCO_3$. The relative activities of phosphatase
566 enzymes appear to correlate with the relative abundances of P_o species identified by ^{31}P NMR
567 e.g. Monoesters > Diesters > Pyro-P.
568 Significant polyphosphate (> 1%) was not detected by ^{31}P NMR during experiments. Previous
569 studies focusing on WWTP tertiary treatment for phosphate removal suggest that redox
570 oscillating conditions promote intracellular poly-P accumulation during aerobic conditions to be
571 used as an energy store under anoxic conditions in order to uptake short chain fatty acids (SCFA)
572 in the absence of an electron acceptor (Hupfer et al., 2007; Wentzel et al., 1991). Phosphate
573 uptake during aerobic conditions therefore requires P availability in excess of what is required
574 for growth and maintenance of the microbial community. However, phosphate availability under
575 aerobic conditions is limited by sorption and coprecipitation with iron oxides, assuming
576 sufficient Fe:P, despite high total phosphorus concentration in sediment. The P requirements by
577 the microbial community are also likely to be high during the transition to aerobic conditions due
578 to the availability of O_2 as an energetically efficient electron acceptor and fermentation products

579 (SCFA), further decreasing the probability of polyphosphate accumulation. Additionally,
580 polyphosphate accumulation and release has shown to be inhibited by denitrification and sulfate
581 reduction due to competition for SCFA (Kortstee et al., 1994; Yamamoto-Ikemoto et al., 1994).

582 ## IMPLICATIONS

583 Our controlled laboratory simulation of highly dynamic redox conditions in eutrophic sediment
584 demonstrates the importance of multiple coupled elemental cycles (C, N, Fe, S, P) when
585 determining internal P loading potential and timing. Our results demonstrate that neither aqueous
586 or solid phase Fe:P ratios or even solid phase P_{Fe} quantification are good predictors of potential P
587 release to the water column under anoxic conditions, due to extensive reversible redistribution of
588 both reduced Fe and associated P within the solid phase. We show that 99.4% of reduced Fe and
589 95.5% of P_{Fe} are not released to the aqueous phase upon Fe reduction but reversibly redistributed
590 within the solid phase upon short periods of iron reduction. Additionally, the apparent
591 requirement for complete nitrate depletion prior to anoxia-promoted P release to the aqueous
592 phase has potential implications for water bodies where significant iron bound legacy P is
593 present within sediments. Our results suggest that decreasing NO_3^- concentrations in external
594 loads, while ostensibly ecologically beneficial, may, in some cases, increase the frequency and
595 magnitude of internal P loading during short periods of anoxia. In P limited systems, the
596 apparent ecological benefits of decreased NO_3^- may be offset by increased P release and
597 eutrophication. However, numerous additional processes exist in natural systems, which were
598 not simulated during our reactor experiment and may influence internal loading mechanisms.
599 Finally, we demonstrate that oscillatory redox conditions, even in sediments with diverse and
600 active microbial communities, do not necessarily result in accumulation of polyphosphate, due to

mineralogical phosphate immobilization and scavenging of SCFA by anaerobic heterotrophic respiration.

Funding Sources

We acknowledge funding from the Canadian Excellence Research Chair (CERC) program and the Water Institute at the University of Waterloo.

Acknowledgements

We would like to acknowledge the support of the Royal Botanical Gardens, particularly Jennifer Bowman and Tys Theymeyer as well as Taylor Maavara who kindly provided her pack raft for use during field sampling. We also acknowledge Jia Cheng (Allen) Yu for his assistance with the production of Figure 1 as well as Marianne Vandergriendt, Kassandra Ma and Christine Ridenour for laboratory assistance.

Abbreviations

Green filamentous algae; GFA, waste water treatment plants; WWTP, sediment-water interface; SWI, dissolved organic carbon; DOC, organic phosphorus species; P_o, soluble reactive phosphorus; SRP, Inductively Coupled Plasma Optical Emission Spectrometry; ICP-OES, organic matter; OM, powder X-ray diffraction; XRD, dissolved reactive phosphorus; DRP, Method detection limit; MDL, non-purgeable organic carbon; NPOC, total dissolved phosphorus; TDP, dissolved inorganic carbon; DIC, relative standard deviation; RSD%, 4-methylumbelliferyl; MUF, 4-Methylumbelliferyl phosphate; MUP, Bis(4-methylumbelliferyl)phosphate; DiMUP, and 4-Methylumbelliferyl pyrophosphate; PYRO-P, 4-

621 Methylumbelliferyl beta-D-glucopyranoside; MUGb, thermo-gravimetric analysis; TGA,

622 terminal electron acceptors; TEAs, particulate organic matter; POM, total phosphorus; TP.

623 ## References

624 4500-P E: Phosphorus by Ascorbic Acid, 1992. , Standard Methods for the Examination of
625 Water and Wastewater. National Water Quality Monitoring Council, Washington, DC,
626 U.S.
627 Aller, R.C., 2004. Conceptual models of early diagenetic processes: The muddy seafloor as an
628 unsteady, batch reactor. J. Mar. Res. 62, 815–835. doi:10.1357/0022240042880837
629 Aller, R.C., 1994. Bioturbation and remineralization of sedimentary organic matter: effects of
630 redox oscillation. Chem. Geol. 114, 331–345. doi:doi: 10.1016/0009-2541(94)90062-0
631 Amirbahman, A., Lake, B.A., Norton, S.A., 2013. Seasonal phosphorus dynamics in the surficial
632 sediment of two shallow temperate lakes: a solid-phase and pore-water study.
633 Hydrobiologia 701, 65–77. doi:10.1007/s10750-012-1257-z
634 Baldwin, D.S., 1996. The phosphorus composition of a diverse series of Australian sediments.
635 Hydrobiologia 335, 63–73. doi:10.1007/BF00013684
636 Berner, R.A., 1977. Stoichiometric models for nutrient regeneration m anoxic sediments1:
637 Nutrient regeneration. Limnol. Oceanogr. 22, 781–786. doi:10.4319/lo.1977.22.5.0781
638 Bonneville, S., Van Cappellen, P., Behrends, T., 2004. Microbial reduction of iron(III)
639 oxyhydroxides: effects of mineral solubility and availability. Chem. Geol. 212, 255–268.
640 doi:doi: 10.1016/j.chemgeo.2004.08.015
641 Bowman, J., Theysmeyer, T., 2014. 2013 RBG Marsh Sediment Quality Assessment (No. Report
642 No. 2014-14). Royal Botanical Gardens, Burlington, Ontario.
643 Cade-Menun, B., 2005. Characterizing phosphorus in environmental and agricultural samples by
644 31P nuclear magnetic resonance spectroscopy. Talanta 66, 359–371.
645 doi:10.1016/j.talanta.2004.12.024
646 Cade-Menun, B.J., Carter, M.R., James, D.C., Liu, C.W., 2010. Phosphorus forms and chemistry
647 in the soil profile under long-term conservation tillage: a phosphorus-31 nuclear magnetic
648 resonance study. J. Environ. Qual. 39, 1647–1656.
649 Cade-Menun, B.J., Navaratnam, J.A., Walbridge, M.R., 2006. Characterizing Dissolved and
650 Particulate Phosphorus in Water with ^{31} P Nuclear Magnetic Resonance Spectroscopy.
651 Environ. Sci. Technol. 40, 7874–7880. doi:10.1021/es061843e
652 Cade-Menun, B.J., Preston, C.M., 1996. A Comparison of Soil Extraction Procedures for 31P
653 NMR Spectroscopy. Soil Sci. 161, 770–785. doi:10.1097/00010694-199611000-00006
654 Caldeira, C.L., Ciminelli, V.S.T., Osseo-Asare, K., 2010. The role of carbonate ions in pyrite
655 oxidation in aqueous systems. Geochim. Cosmochim. Acta 74, 1777–1789. doi:doi:
656 10.1016/j.gca.2009.12.014
657 Caraco, N.F., Cole, J.J., Likens, G.E., 1989. Evidence for sulphate-controlled phosphorus release
658 from sediments of aquatic systems. Nature 341, 316–318. doi:10.1038/341316a0
659 Chorover, J., Amistadi, M.K., 2001. Reaction of forest floor organic matter at goethite, birnessite
660 and smectite surfaces. Geochim. Cosmochim. Acta 65, 95–109. doi:10.1016/S0016-
661 7037(00)00511-1

662 Chow-Fraser, P., Lougheed, V., Le Thiec, V., Crosbie, B., Simser, L., Lord, J., 1998. Long-term
663 response of the biotic community to fluctuating water levels and changes in water quality
664 in Cootes Paradise Marsh, a degraded coastal wetland of Lake Ontario. Wetl. Ecol.
665 Manag. 6, 19–42. doi:10.1023/A:1008491520668
666 Chun, C.L., Ochsner, U., Byappanahalli, M.N., Whitman, R.L., Tepp, W.H., Lin, G., Johnson,
667 E.A., Peller, J., Sadowsky, M.J., 2013. Association of Toxin-Producing *Clostridium*
668 *botulinum* with the Macroalga *Cladophora* in the Great Lakes. Environ. Sci. Technol. 47,
669 2587–2594. doi:10.1021/es304743m
670 Cline, J.D., 1969. Spectrophotometric determination of hydrogen sulfide in natural waters.
671 Limnol. Oceanogr. 14, 454–458. doi:10.4319/lo.1969.14.3.0454
672 Conley, D.J., Paerl, H.W., Howarth, R.W., Boesch, D.F., Seitzinger, S.P., Havens, K.E.,
673 Lancelot, C., Likens, G.E., 2009. ECOLOGY: Controlling Eutrophication: Nitrogen and
674 Phosphorus. Science 323, 1014–1015. doi:10.1126/science.1167755
675 Corazza, C., Tironi, S., 2011. European Parliament supports ban of phosphates in consumer
676 detergents (Press Release No. IP/11/1542). European Commission, Brussels, Belgium.
677 D. Krom, M., A. Berner, R., 1981. The diagenesis of phosphorus in a nearshore marine sediment.
678 Geochim. Cosmochim. Acta 45, 207–216. doi:10.1016/0016-7037(81)90164-2
679 DeAngelis, K.M., Silver, W.L., Thompson, A.W., Firestone, M.K., 2010. Microbial communities
680 acclimate to recurring changes in soil redox potential status. Environ. Microbiol. 12,
681 3137–3149. doi:10.1111/j.1462-2920.2010.02286.x
682 Deng, S., Popova, I.E., Dick, L., Dick, R., 2013. Bench scale and microplate format assay of soil
683 enzyme activities using spectroscopic and fluorometric approaches. Appl. Soil Ecol. 64,
684 84–90. doi:10.1016/j.apsoil.2012.11.002
685 Doolette, A.L., Smernik, R.J., Dougherty, W.J., 2009. Spiking Improved Solution Phosphorus-31
686 Nuclear Magnetic Resonance Identification of Soil Phosphorus Compounds. Soil Sci.
687 Soc. Am. J. 73, 919. doi:10.2136/sssaj2008.0192
688 Dunn, C., Jones, T.G., Girard, A., Freeman, C., 2013. Methodologies for Extracellular Enzyme
689 Assays from Wetland Soils. Wetlands 34, 9–17. doi:10.1007/s13157-013-0475-0
690 Einsele, W., 1936. Über die Beziehungen des Eisenkreislaufs zum Phosphatkreislauf im
691 eutrophen See. Arch Hydrobiol 29, 664–686.
692 Fisher, J.B., Lick, W.J., McCall, P.L., Robbins, J.A., 1980. Vertical mixing of lake sediments by
693 tubificid oligochaetes. J. Geophys. Res. 85, 3997. doi:10.1029/JC085iC07p03997
694 Frohne, T., Rinklebe, J., Diaz-Bone, R.A., Du Laing, G., 2011. Controlled variation of redox
695 conditions in a floodplain soil: Impact on metal mobilization and biomethylation of
696 arsenic and antimony. Geoderma 160, 414–424. doi:doi:
697 10.1016/j.geoderma.2010.10.012
698 Furukawa, Y., Bentley, S.J., Lavoie, D.L., 2001. Bioirrigation modeling in experimental benthic
699 mesocosms. J. Mar. Res. 59, 417–452. doi:10.1357/002224001762842262
700 Gächter, R., Meyer, J.S., 1993. The role of microorganisms in mobilization and fixation of
701 phosphorus in sediments. Hydrobiologia 253, 103–121. doi:10.1007/BF00050731
702 Gächter, R., Meyer, J.S., Mares, A., 1988. Contribution of bacteria to release and fixation of
703 phosphorus in lake sediments: Bacteria and P in sediments. Limnol. Oceanogr. 33, 1542–
704 1558. doi:10.4319/lo.1988.33.6part2.1542
705 Gächter, R., Müller, B., 2003. Why the Phosphorus Retention of Lakes Does Not Necessarily
706 Depend on the Oxygen Supply to Their Sediment Surface. Limnol. Oceanogr. 48, 929–
707 933. doi:10.2307/3096591

708 Gardner, W.H., 1986. Water Content, in: Methods of Soil Analysis: Physical and Mineralogical
709 Methods, Agronomy. Soil Science Society of America, Madison, Wisconsin, pp. 493–
710 544.
711 Gehin, A., Greneche, J.-M., Tournassat, C., Brendle, J., Rancourt, D.G., Charlet, L., 2007.
712 Reversible surface-sorption-induced electron-transfer oxidation of Fe(II) at reactive sites
713 on a synthetic clay mineral. Geochim. Cosmochim. Acta 71, 863–876. doi:doi:
714 10.1016/j.gca.2006.10.019
715 Gerke, J., 2010. Humic (Organic Matter)-Al(Fe)-Phosphate Complexes: An Underestimated
716 Phosphate Form in Soils and Source of Plant-Available Phosphate. Soil Sci. 175, 417–
717 425. doi:10.1097/SS.0b013e3181f1b4dd
718 Gerke, J., 1993. Phosphate adsorption by humic/Fe-oxide mixtures aged at pH 4 and 7 and by
719 poorly ordered Fe-oxide. Geoderma 59, 279–288. doi:10.1016/0016-7061(93)90074-U
720 Gorham, E., Boyce, F.M., 1989. Influence of Lake Surface Area and Depth Upon Thermal
721 Stratification and the Depth of the Summer Thermocline. J. Gt. Lakes Res. 15, 233–245.
722 doi:10.1016/S0380-1330(89)71479-9
723 Grybos, M., Davranche, M., Gruau, G., Petitjean, P., Pedrot, M., 2009. Increasing pH drives
724 organic matter solubilization from wetland soils under reducing conditions. Geoderma
725 154, 13–19. doi:doi: DOI: 10.1016/j.geoderma.2009.09.001
726 Hansen, J.C., Cade-Menun, B.J., Strawn, D.G., 2004. Phosphorus Speciation in Manure-
727 Amended Alkaline Soils. J. Environ. Qual. 33, 1521. doi:10.2134/jeq2004.1521
728 Hedley, M.J., White, R.E., Nye, P.H., 1982. Plant-Induced changes in the rhizosphere of rape
729 (Brassica Napus Var.Emerald) seedlings. III. Changes in L value, soil phosphate fractions
730 and phosphatase activity. New Phytol. 91, 45–56. doi:10.1111/j.1469-
731 8137.1982.tb03291.x
732 Hölker, F., Vanni, M.J., Kuiper, J.J., Meile, C., Grossart, H.-P., Stief, P., Adrian, R., Lorke, A.,
733 Dellwig, O., Brand, A., Hupfer, M., Mooij, W.M., Nützmann, G., Lewandowski, J., 2015.
734 Tube-dwelling invertebrates: tiny ecosystem engineers have large effects in lake
735 ecosystems. Ecol. Monogr. 85, 333–351. doi:10.1890/14-1160.1
736 Hongve, D., 1997. Cycling of iron, manganese, and phosphate in a meromictic lake. Limnol.
737 Oceanogr. 42, 635–647. doi:10.4319/lo.1997.42.4.0635
738 Hupfer, M., Gloess, S., Grossart, H., 2007. Polyphosphate-accumulating microorganisms in
739 aquatic sediments. Aquat. Microb. Ecol. 47, 299–311. doi:10.3354/ame047299
740 Hyacinthe, C., Van Cappellen, P., 2004. An authigenic iron phosphate phase in estuarine
741 sediments: composition, formation and chemical reactivity. Mar. Chem. 91, 227–251.
742 doi:10.1016/j.marchem.2004.04.006
743 Jensen, D.L., Boddum, J.K., Tjell, J.C., Christensen, T.H., 2002. The solubility of rhodochrosite
744 (MnCO3) and siderite (FeCO3) in anaerobic aquatic environments. Appl. Geochem. 17,
745 503–511. doi:doi: DOI: 10.1016/S0883-2927(01)00118-4
746 Jensen, H.S., Kristensen, P., Jeppesen, E., Skytthe, A., 1992. Iron:phosphorus ratio in surface
747 sediment as an indicator of phosphate release from aerobic sediments in shallow lakes.
748 Hydrobiologia 235–236, 731–743. doi:10.1007/BF00026261
749 Jørgensen, C., Inglett, K.S., Jensen, H.S., Reitzel, K., Reddy, K.R., 2015. Characterization of
750 biogenic phosphorus in outflow water from constructed wetlands. Geoderma 257–258,
751 58–66. doi:10.1016/j.geoderma.2015.01.019
752 Joshi, S.R., Kukkadapu, R.K., Burdige, D.J., Bowden, M.E., Sparks, D.L., Jaisi, D.P., 2015.
753 Organic Matter Remineralization Predominates Phosphorus Cycling in the Mid-Bay

754 Sediments in the Chesapeake Bay. Environ. Sci. Technol. 49, 5887–5896.
755 doi:10.1021/es5059617
756 Kang, H., Freeman, C., 1999. Phosphatase and arylsulphatase activities in wetland soils: annual
757 variation and controlling factors. Soil Biol. Biochem. 31, 449–454. doi:10.1016/S0038-
758 0717(98)00150-3
759 Katsev, S., Tsandev, I., L'Heureux, I., Rancourt, D.G., 2006. Factors controlling long-term
760 phosphorus efflux from lake sediments: Exploratory reactive-transport modeling. Chem.
761 Geol. 234, 127–147. doi:10.1016/j.chemgeo.2006.05.001
762 Kim, D.-K., Zhang, W., Rao, Y.R., Watson, S., Mugalingam, S., Labencki, T., Dittrich, M.,
763 Morley, A., Arhonditsis, G.B., 2013. Improving the representation of internal nutrient
764 recycling with phosphorus mass balance models: A case study in the Bay of Quinte,
765 Ontario, Canada. Ecol. Model. 256, 53–68. doi:10.1016/j.ecolmodel.2013.02.017
766 Kizewski, F.R., Boyle, P., Hesterberg, D., Martin, J.D., 2010a. Mixed Anion
767 (Phosphate/Oxalate) Bonding to Iron(III) Materials. J. Am. Chem. Soc. 132, 2301–2308.
768 doi:10.1021/ja908807b
769 Kizewski, F.R., Hesterberg, D., Martin, J., 2010b. Phosphate sorption to organic
770 matter/ferrihydrite systems as affected by aging time. Presented at the 19th World
771 Congress of Soil Science, Soil Solutions for a Changing World, Brisbane, Australia.
772 Klein, A.R., Baldwin, D.S., Singh, B., Silvester, E.J., 2010. Salinity-induced acidification in a
773 wetland sediment through the displacement of clay-bound iron(II). Environ. Chem. 7,
774 413. doi:10.1071/EN10057
775 Kortstee, G.J.J., Appeldoorn, K.J., Bonting, C.F.C., Niel, E.W.J., Veen, H.W., 1994. Biology of
776 polyphosphate-accumulating bacteria involved in enhanced biological phosphorus
777 removal. FEMS Microbiol. Rev. 15, 137–153. doi:10.1111/j.1574-6976.1994.tb00131.x
778 Lagauzère, S., Boyer, P., Stora, G., Bonzom, J.-M., 2009. Effects of uranium-contaminated
779 sediments on the bioturbation activity of Chironomus riparius larvae (Insecta, Diptera)
780 and Tubifex tubifex worms (Annelida, Tubificidae). Chemosphere 76, 324–334.
781 doi:10.1016/j.chemosphere.2009.03.062
782 Li, W., Joshi, S.R., Hou, G., Burdige, D.J., Sparks, D.L., Jaisi, D.P., 2015. Characterizing
783 Phosphorus Speciation of Chesapeake Bay Sediments Using Chemical Extraction, ^{31} P
784 NMR, and X-ray Absorption Fine Structure Spectroscopy. Environ. Sci. Technol. 49,
785 203–211. doi:10.1021/es504648d
786 Liger, E., Charlet, L., Van Cappellen, P., 1999. Surface catalysis of uranium(VI) reduction by
787 iron(II). Geochim. Cosmochim. Acta 63, 2939–2955. doi:doi: DOI: 10.1016/S0016-
788 7037(99)00265-3
789 Mallin, M.A., McIver, M.R., Wells, H.A., Parsons, D.C., Johnson, V.L., 2005. Reversal of
790 eutrophication following sewage treatment upgrades in the New River Estuary, North
791 Carolina. Estuaries 28, 750–760. doi:10.1007/BF02732912
792 Manning, B.A., 1996. Modeling Arsenate Competitive Adsorption on Kaolinite, Montmorillonite
793 and Illite. Clays Clay Miner. 44, 609–623. doi:10.1346/CCMN.1996.0440504
794 Matisoff, G., Kaltenberg, E.M., Steely, R.L., Hummel, S.K., Seo, J., Gibbons, K.J., Bridgeman,
795 T.B., Seo, Y., Behbahani, M., James, W.F., Johnson, L.T., Doan, P., Dittrich, M., Evans,
796 M.A., Chaffin, J.D., 2016. Internal loading of phosphorus in western Lake Erie. J. Gt.
797 Lakes Res. 42, 775–788. doi:10.1016/j.jglr.2016.04.004
798 Matisoff, G., Wang, X., 1998. Solute transport in sediments by freshwater infaunal bioirrigators.
799 Limnol. Oceanogr. 43, 1487–1499. doi:10.4319/lo.1998.43.7.1487

800 Mayer, T., Rosa, F., Mayer, R., Charlton, M., 2006. Relationship Between the Sediment
801 Geochemistry and Phosphorus Fluxes in a Great Lakes Coastal Marsh, Cootes Paradise,
802 ON, Canada. Water Air Soil Pollut. Focus 6, 495–503. doi:10.1007/s11267-006-9033-6
803 McCall, P.L., Fisher, J.B., 1980. Effects of Tubificid Oligochaetes on Physical and Chemical
804 Properties of Lake Erie Sediments, in: Brinkhurst, R., Cook, D. (Eds.), Aquatic
805 Oligochaete Biology. Springer US, pp. 253–317.
806 McLaughlin, C., Pike, K., 2014. Muddied Waters: The Ongoing Challenge of Sediment and
807 Phosphorus for Hamilton Harbour Remediation (2014 Towards Safe Harbour Report).
808 Bay Area Restoration Council, Hamilton, Ontario.
809 Mikutta, C., Kretzschmar, R., 2011. Spectroscopic Evidence for Ternary Complex Formation
810 between Arsenate and Ferric Iron Complexes of Humic Substances. Environ. Sci.
811 Technol. 45, 9550–9557. doi:10.1021/es202300w
812 Mortimer, C.H., 1971. Chemical Exchanges Between Sediments and Water in the Great Lakes-
813 Speculations on Probable Regulatory Mechanisms. Limnol. Oceanogr. 16, 387–404.
814 doi:10.2307/2834170
815 Mortimer, C.H., 1941. The exchange of dissolved substances between mud and water in lakes. J.
816 Ecol. 29, 280–329.
817 Murphy, J., Riley, J.P., 1962. A modified single solution method for the determination of
818 phosphate in natural waters. Anal. Chim. Acta 27, 31–36. doi:10.1016/S0003-
819 2670(00)88444-5
820 Nikolausz, M., Kappelmeyer, U., Szekely, A., Rusznyak, A., Marialigeti, K., Kastner, M., 2008.
821 Diurnal redox fluctuation and microbial activity in the rhizosphere of wetland plants. Eur.
822 J. Soil Biol. 44, 324–333. doi:doi: DOI: 10.1016/j.ejsobi.2008.01.003
823 Nürnberg, G.K., 1988. Prediction of Phosphorus Release Rates from Total and Reductant-
824 Soluble Phosphorus in Anoxic Lake Sediments. Can. J. Fish. Aquat. Sci. 45, 453–462.
825 doi:10.1139/f88-054
826 O'Connell, D.W., Jensen, M.M., Jakobsen, R., Thamdrup, B., Andersen, T.J., Kovacs, A.,
827 Hansen, H.C.B., 2015. Vivianite formation and its role in phosphorus retention in Lake
828 Ørn, Denmark. Chem. Geol. doi:10.1016/j.chemgeo.2015.05.002
829 Olsen, S.R., Cole, C.V., Watanabe, F.S., Dean, L.A., 1954. Estimation of available phosphorus
830 in soils by extraction with sodium bicarbonate. US Dep Agric Circ 939, 1–19.
831 Olsen, S.R., Watanabe, F.S., 1957. A Method to Determine a Phosphorus Adsorption Maximum
832 of Soils as Measured by the Langmuir Isotherm1. Soil Sci. Soc. Am. J. 21, 144.
833 doi:10.2136/sssaj1957.03615995002100020004x
834 Painter, D.., Hampton, L., Simser, W.L., 1991. Cootes Paradise Water Turbidity: Sources and
835 Recommendations., in: NWRI Contribution Paper #91-15. Burlington, Ontario, p. 18.
836 Pallasser, R., Minasny, B., McBratney, A.B., 2013. Soil carbon determination by
837 thermogravimetrics. PeerJ 1, e6. doi:10.7717/peerj.6
838 Paraskova, J.V., Jørgensen, C., Reitzel, K., Pettersson, J., Rydin, E., Sjöberg, P.J.R., 2015.
839 Speciation of Inositol Phosphates in Lake Sediments by Ion-Exchange Chromatography
840 Coupled with Mass Spectrometry, Inductively Coupled Plasma Atomic Emission
841 Spectroscopy, and ^{31} P NMR Spectroscopy. Anal. Chem. 87, 2672–2677.
842 doi:10.1021/ac5033484
843 Parkhurst, D.L., Appelo, C.A.J., (US), G.S., 1999. User's guide to PHREEQC (Version 3): A
844 computer program for speciation, batch-reaction, one-dimensional transport, and inverse
845 geochemical calculations. US Geological Survey Reston, VA.

846 Parsons, C.T., Couture, R.-M., Omoregie, E.O., Bardelli, F., Greneche, J.-M., Roman-Ross, G.,
847 Charlet, L., 2013. The impact of oscillating redox conditions: Arsenic immobilisation in
848 contaminated calcareous floodplain soils. Environ. Pollut. 178, 254–263.
849 doi:10.1016/j.envpol.2013.02.028
850 Peiffer, S., Behrends, T., Hellige, K., Larese-Casanova, P., Wan, M., Pollok, K., 2015. Pyrite
851 formation and mineral transformation pathways upon sulfidation of ferric hydroxides
852 depend on mineral type and sulfide concentration. Chem. Geol. 400, 44–55.
853 doi:10.1016/j.chemgeo.2015.01.023
854 Pelegri, S.P., Blackburn, T.H., 1995. Effects of Tubifex tubifex (Oligochaeta: Tubificidae) on N-
855 mineralization in freshwater sediments, measured with isotopes. Aquat. Microb. Ecol. 9,
856 289–294.
857 Penn, M.R., Auer, M.T., Doerr, S.M., Driscoll, C.T., Brooks, C.M., Effler, S.W., 2000.
858 Seasonality in phosphorus release rates from the sediments of a hypereutrophic lake
859 under a matrix of pH and redox conditions. Can. J. Fish. Aquat. Sci. 57, 1033–1041.
860 doi:10.1139/f00-035
861 Phillips, G., Jackson, R., Bennett, C., Chilvers, A., 1994. The importance of sediment
862 phosphorus release in the restoration of very shallow lakes (The Norfolk Broads,
863 England) and implications for biomanipulation. Hydrobiologia 275–276, 445–456.
864 doi:10.1007/BF00026733
865 Pomeroy, R., 1954. Auxiliary Pretreatment by Zinc Acetate in Sulfide Analyses. Anal. Chem.
866 26, 571–572. doi:10.1021/ac60087a047
867 Pretty, J.N., Mason, C.F., Nedwell, D.B., Hine, R.E., Leaf, S., Dils, R., 2003. Environmental
868 Costs of Freshwater Eutrophication in England and Wales. Environ. Sci. Technol. 37,
869 201–208. doi:10.1021/es020793k
870 Reddy, K.R., DeLaune, R.D., 2008. Biogeochemistry of wetlands: science and applications.
871 CRC Press, Boca Raton.
872 Reddy, K.R., Newman, S., Osborne, T.Z., White, J.R., Fitz, H.C., 2011. Phosphorous Cycling in
873 the Greater Everglades Ecosystem: Legacy Phosphorous Implications for Management
874 and Restoration. Crit. Rev. Environ. Sci. Technol. 41, 149–186.
875 doi:10.1080/10643389.2010.530932
876 Reitzel, K., Ahlgren, J., DeBrabandere, H., Waldebäck, M., Gogoll, A., Tranvik, L., Rydin, E.,
877 2007. Degradation rates of organic phosphorus in lake sediment. Biogeochemistry 82,
878 15–28. doi:10.1007/s10533-006-9049-z
879 Rezanezhad, F., Couture, R.-M., Kovac, R., O'Connell, D., Van Cappellen, P., 2014. Water table
880 fluctuations and soil biogeochemistry: An experimental approach using an automated soil
881 column system. J. Hydrol. 509, 245–256. doi:10.1016/j.jhydrol.2013.11.036
882 Rickard, D., Morse, J.W., 2005. Acid volatile sulfide (AVS). Mar. Chem. 97, 141–197.
883 doi:10.1016/j.marchem.2005.08.004
884 Routledge, I., 2012. City of Hamilton: King Street (Dundas) Wastewater Treatment Plant. 2011
885 Annual Report (Annual Report No. Works Number 120001372). The City of Hamilton,
886 Environment and Sustainable Infrastructure Division, Hamilton, Ontario.
887 Ruttenberg, K.C., 1992. Development of a sequential extraction method for different forms of
888 phosphorus in marine sediments. Limnol. Oceanogr. 37, 1460–1482.
889 doi:10.4319/lo.1992.37.7.1460

890 Sannigrahi, P., Ingall, E., 2005. Polyphosphates as a source of enhanced P fluxes in marine
891 sediments overlain by anoxic waters: Evidence from [sup 31]P NMR. Geochem. Trans. 6,
892 52. doi:10.1063/1.1946447
893 Semkin, R.G., McLarty, A.W., Craig, D., 1976. A water quality study of Cootes Paradise.
894 Ontario Ministry of Environment, West Central Region, Toronto, Ontario.
895 Sharma, P., Ofner, J., Kappler, A., 2010. Formation of Binary and Ternary Colloids and
896 Dissolved Complexes of Organic Matter, Fe and As. Environ. Sci. Technol. 44, 4479–
897 4485. doi:10.1021/es100066s
898 Sharpley, A.N., Chapra, S.C., Wedepohl, R., Sims, J.T., Daniel, T.C., Reddy, K.R., 1994.
899 Managing Agricultural Phosphorus for Protection of Surface Waters: Issues and Options.
900 J. Environ. Qual. 23, 437. doi:10.2134/jeq1994.00472425002300030006x
901 Sibanda, H.M., Young, S.D., 1986. Competitive adsorption of humus acids and phosphate on
902 goethite, gibbsite and two tropical soils. J. Soil Sci. 37, 197–204. doi:10.1111/j.1365-
903 2389.1986.tb00020.x
904 Sirová, D., Rejmánková, E., Carlson, E., Vrba, J., 2013. Current standard assays using artificial
905 substrates overestimate phosphodiesterase activity. Soil Biol. Biochem. 56, 75–79.
906 doi:10.1016/j.soilbio.2012.02.008
907 Smith, V.H., Schindler, D.W., 2009. Eutrophication science: where do we go from here? Trends
908 Ecol. Evol. 24, 201–207. doi:10.1016/j.tree.2008.11.009
909 Søndergaard, M., Jensen, J.P., Jeppesen, E., 2003. Role of sediment and internal loading of
910 phosphorus in shallow lakes. Hydrobiologia 506–509, 135–145.
911 doi:10.1023/B:HYDR.0000008611.12704.dd
912 Song, K.-Y., Zoh, K.-D., Kang, H., 2007. Release of phosphate in a wetland by changes in
913 hydrological regime. Sci. Total Environ. 380, 13–18. doi:10.1016/j.scitotenv.2006.11.035
914 Stookey, L.L., 1970. Ferrozine - a new spectrophotometric reagent for iron. Anal. Chem. 42,
915 779–781. doi:doi: 10.1021/ac60289a016
916 Stumm, W., Morgan, J.J., 1996. Aquatic Chemistry, 3rd ed. ed. John Wiley & Sons, New York
917 [etc.].
918 Theysmeyer, T., Smith, T., Simser, L., 1999. West Pond 1999 Study. Royal Botanical Gardens,
919 Science Department.
920 Thibault, P.-J., Rancourt, D.G., Evans, R.J., Dutrizac, J.E., 2009. Mineralogical confirmation of
921 a near-P:Fe=1:2 limiting stoichiometric ratio in colloidal P-bearing ferrihydrite-like
922 hydrous ferric oxide. Geochim. Cosmochim. Acta 73, 364–376.
923 doi:10.1016/j.gca.2008.10.031
924 Thompson, A., Chadwick, O.A., Rancourt, D.G., Chorover, J., 2006. Iron-oxide crystallinity
925 increases during soil redox oscillations. Geochim. Cosmochim. Acta 70, 1710–1727.
926 doi:10.1016/j.gca.2005.12.005
927 Turner, B.L., Cade-Menun, B.J., Westermann, D.T., 2003a. Organic phosphorus composition
928 and potential bioavailability in semi-arid arable soils of the Western United States. Soil
929 Sci. Soc. Am. J. 67, 1168–1179.
930 Turner, B.L., Mahieu, N., Condron, L., 2003b. Phosphorus-31 Nuclear Magnetic Resonance
931 Spectral Assignments of Phosphorus Compounds in Soil NaOH–EDTA Extracts. Soil
932 Sci. Soc. Am. J. 67, 497. doi:10.2136/sssaj2003.4970
933 U.S. EPA, 9/99. Field Sampling Guidance Document: Sediment Sampling (No. #1215). U.S.
934 Environmental Protection Agency. Region 9 Laboratory, Richmond California.

Vetter, Y.A., Deming, J.W., Jumars, P.A., Krieger-Brockett, B.B., 1998. A Predictive Model of Bacterial Foraging by Means of Freely Released Extracellular Enzymes. Microb. Ecol. 36, 75–92. doi:10.1007/s002489900095

Viollier, E., Inglett, P.., Hunter, K., Roychoudhury, A.., Van Cappellen, P., 2000. The ferrozine method revisited: Fe(II)/Fe(III) determination in natural waters. Appl. Geochem. 15, 785–790. doi:10.1016/S0883-2927(99)00097-9

Weishaar, J.L., Aiken, G.R., Bergamaschi, B.A., Fram, M.S., Fujii, R., Mopper, K., 2003. Evaluation of Specific Ultraviolet Absorbance as an Indicator of the Chemical Composition and Reactivity of Dissolved Organic Carbon. Environ. Sci. Technol. 37, 4702–4708. doi:10.1021/es030360x

Wentzel, M.C., Lötter, L.H., Ekama, G.A., Loewenthal, R.E., Marais, G. v R., 1991. Evaluation of Biochemical Models for Biological Excess Phosphorus Removal. Water Sci. Technol. 23, 567–576.

Yamamoto-Ikemoto, R., Matsui, S., Komori, T., 1994. Ecological interactions among denitrification, poly-P accumulation, sulfate reduction, and filamentous sulfur bacteria in activated sludge. Water Sci. Technol. 30, 201–210.

Tables

Step	Extractant	Conditions	Target phase
1a	1M $MgCl_2$	pH 8 for 2 hours @ 25ºC	Exchangeable or Loosely sorbed P (P_{Ex})
1b	1M $MgCl_2$	pH 8 for 2 hours @ 25ºC	
1c	18.2 MΩ cm^{-1} H_2O	2 hours @ 25ºC	
2a	1M $NaHCO_3$	pH 7.6 for 16 hours @ 25ºC	Organic associated P (P_{Hum})
2b	1M $NaHCO_3$	pH 7.6 for 2 hours @ 25ºC	
2c	1M $NaHCO_3$	pH 7.6 for 2 hours @ 25ºC	
2d	1M $NaHCO_3$	pH 7.6 for 2 hours @ 25ºC	
2e	1M $MgCl_2$	pH 8 for 2 hours @ 25ºC	
3a	0.3 M Na_3-citrate with 1M $NaHCO_3$ with 1.125g of Na-ditionite (CDB)	pH 7.6 for 8 hours @ 25ºC	Fe-bound P (P_{Fe})
3b	CDB	pH 7.6 for 2 hours @ 25ºC	
3c	1M $MgCl_2$	pH 8 for 2 hours @ 25ºC	
4a	1M Na-acetate with acetic acid	pH 4 for 6 hours @ 25ºC	Authigenic carbonate fluorapatite plus biogenic apatite plus $CaCO_3$-bound P (P_{CFA})
4b	1M Na-acetate with acetic acid	pH 4 for 2 hours @ 25ºC	
4c	1M $MgCl_2$	pH 8 for 2 hours @ 25ºC	
5	1M HCl	16 hours @ 25ºC	Detrital Apatite plus other inorganic-P (P_{Detri})

6	1M HCl	16 hours after ashing at 550°C @ 25°C	Residual/Organic-P (P_{Resi})

953

954 *Table 1: Summary of the modified SEDEX sequential extraction protocol used on*
955 *solid samples taken over a time series during the reactor experiment. Results of*
956 *this extraction are shown in Figure 4.*

957 **Figures**

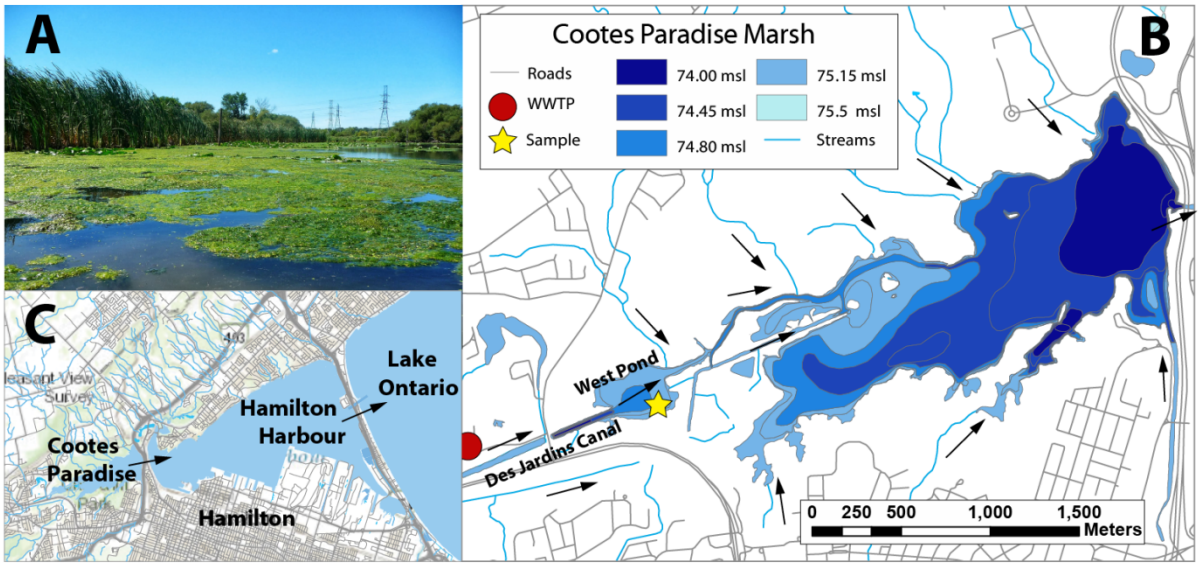

958

959 *Figure 1: A) Photograph of the sampling location taken on the day of sampling*
960 *illustrating the abundance of green filamentous algae. B) Map of Cootes Paradise*
961 *and West Pond showing the sampling location, local hydrological network and the*
962 *King Street Waste Water Treatment plant in Dundas. Color represents area*
963 *covered by surface water at different water levels (msl= meters above sea level)*
964 *C) Overview map showing the hydrological connection between Cootes Paradise,*
965 *Hamilton Harbour and Lake Ontario.*

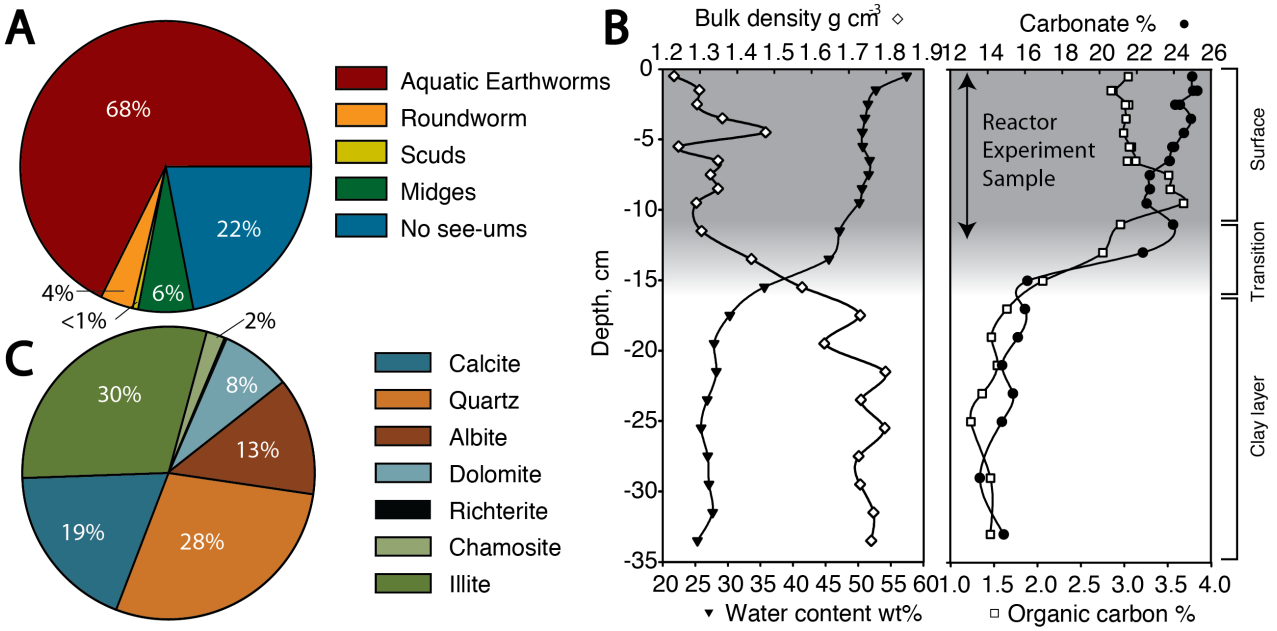

966
967 *Figure 2: a) Proportions of bioturbating macro invertebrates identified in the top*
968 *18 cm b) Depth profiles of sampled sediment, water content weight % (inverted*
969 *black triangles), bulk density (white diamonds) OM % (white squares), carbonate*
970 *% (black circles) c) Mineralogical composition of sediments from the zone of*
971 *bioturbation determined by XRD (top 12 cm).*

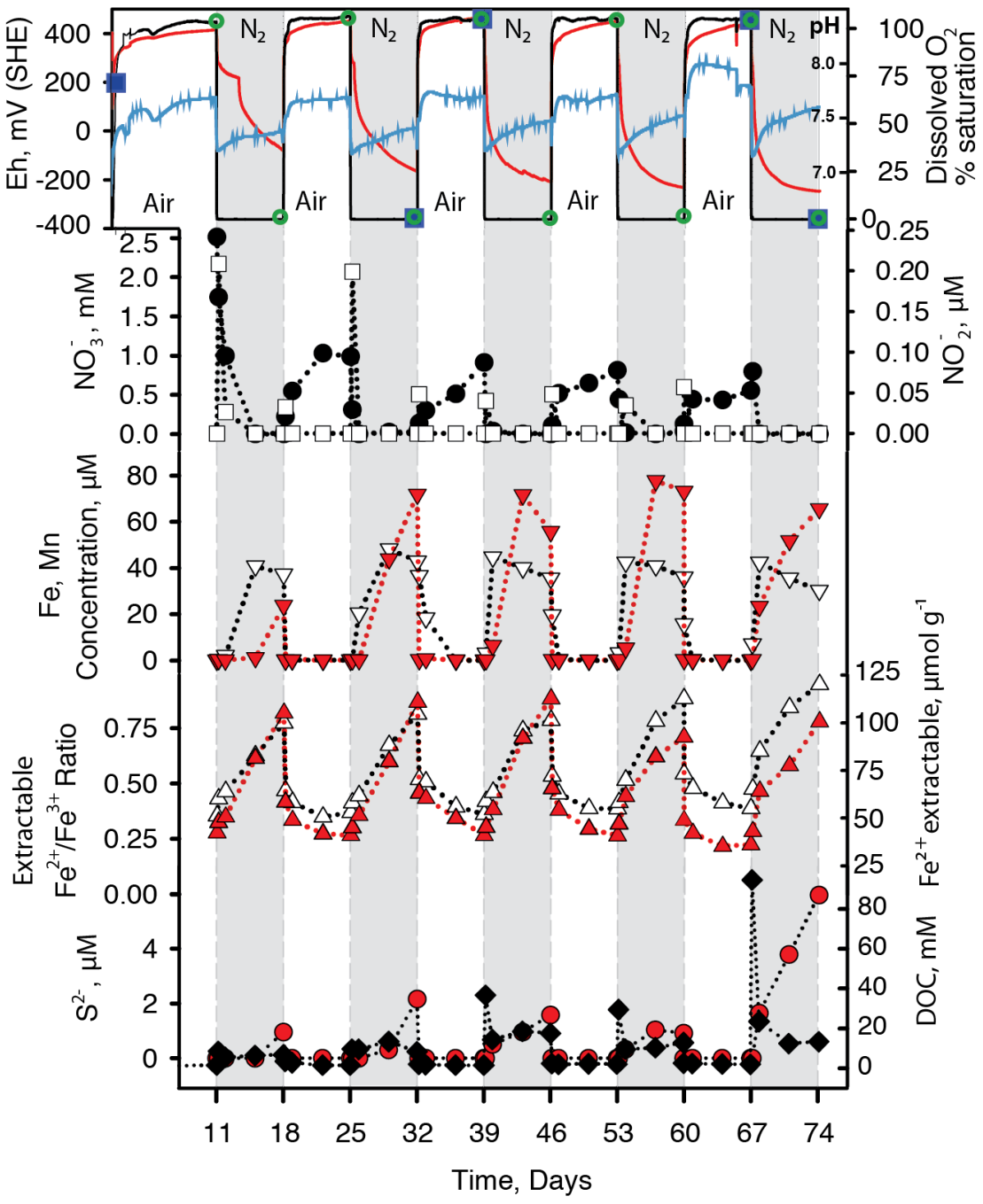

Figure 3: Aqueous chemistry and iron extraction data with time during reactor experiments: Solid red line = E_h, solid black line = DO, solid blue line = pH, full black circles = NO_3^-, white squares = NO_2^-, inverted red triangles = $Fe_{(aq)}$, inverted white triangles = $Mn_{(aq)}$, red triangles = Fe^{2+} 0.5M HCl extractable, white triangles

977 *= Fe^{2+}/Fe^{3+} ratio in 0.5M HCl extract, red circles = S_2^-, black diamonds = DOC.*

978 *Sampling points for ^{31}P NMR and extracellular enzyme assays (EEA) are shown on*

979 *the E_h curve (^{31}P NMR = open blue squares, EEA = open green circles).*

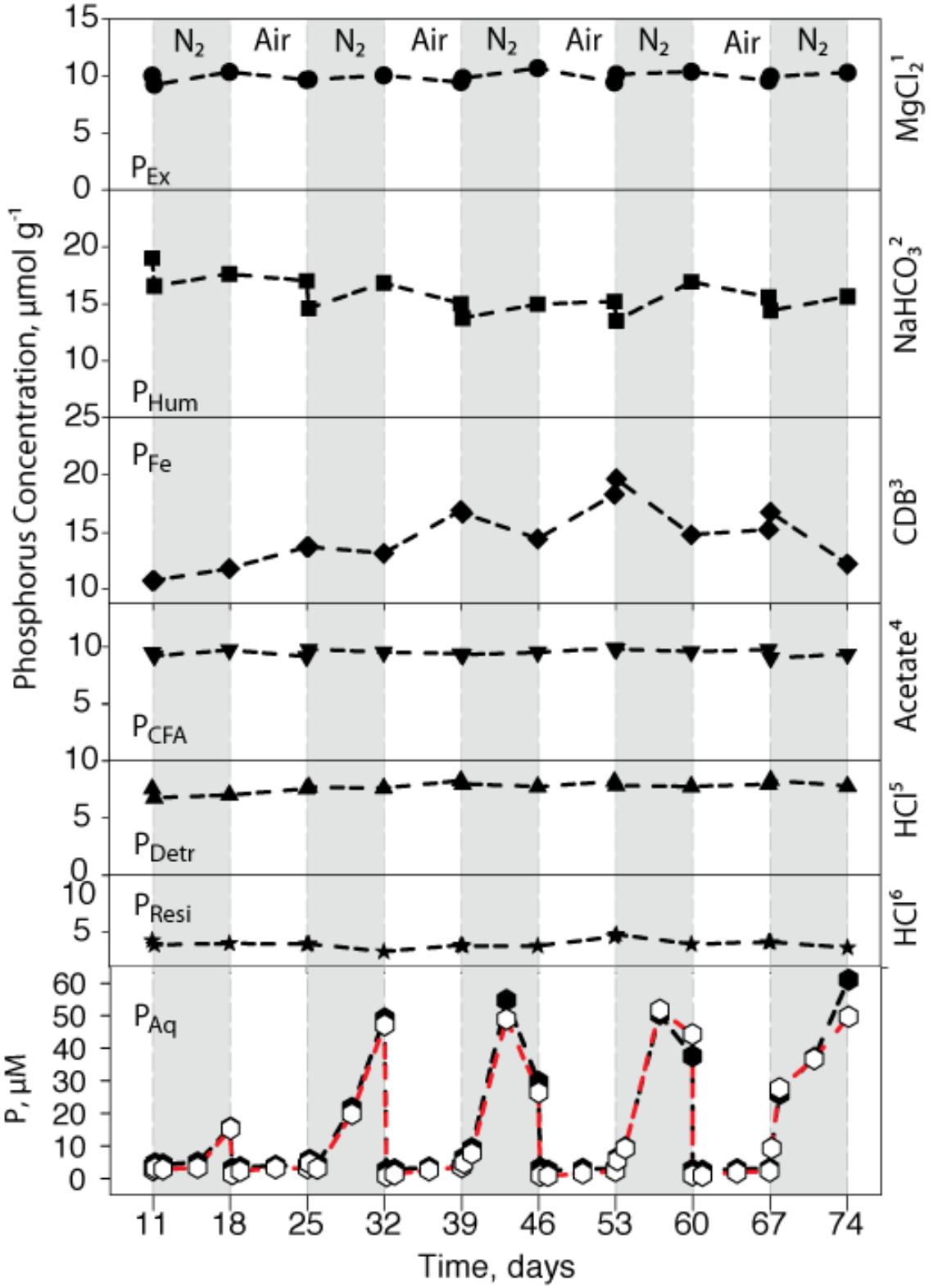

980
981 *Figure 4: Aqueous and solid phase phosphorus speciation from sequential*
982 *chemical extractions with time during the reactor experiment. White panels*

correspond to time periods with air sparging, grey panels correspond to time periods with N_2:CO_2 sparging. Black symbols = total P concentration, white symbols = SRP concentration.

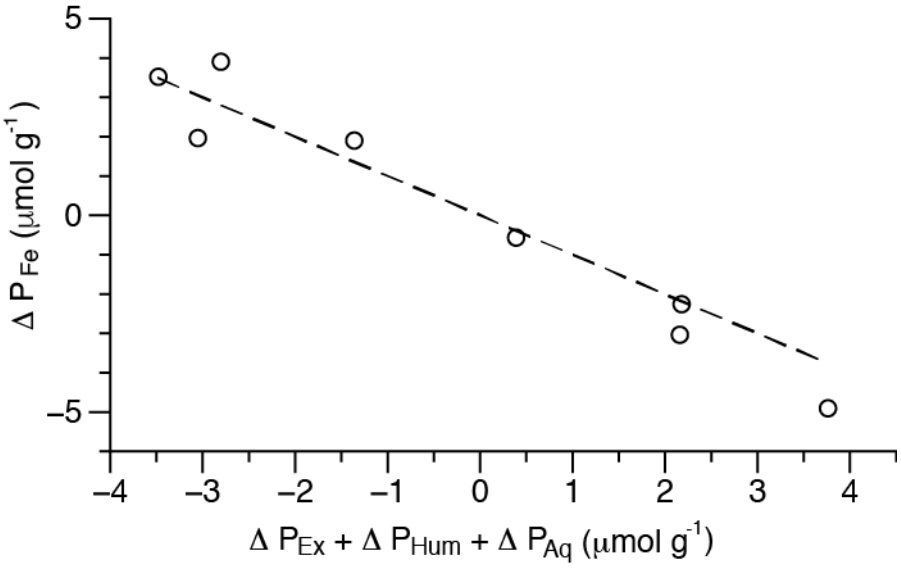

Figure 5: Change in P distribution between the start and end of each oxic and anoxic period (7 day change). Iron-bound P (P_{Fe}) appears to be reversibly redistributed to the loosely sorbed (P_{Ex}), humic bound (P_{Hum}) and aqueous fractions (P_{Aq}). The dashed line is 1:1. Linear regression of the data results in an R^2 of 0.95, a slope of -1.1 and $p < 0.0001$).

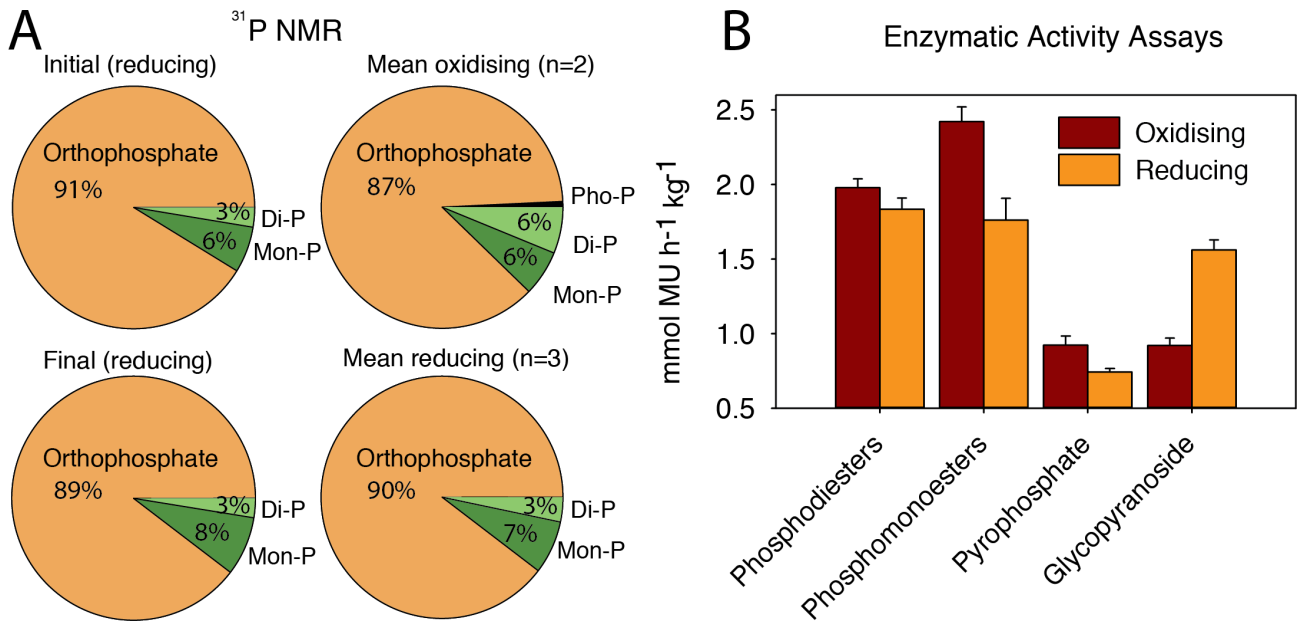

Figure 6: A) P speciation determined by ^{31}P NMR for the initial suspension (top left), the final suspension (bottom left), the average of samples from oxic conditions n=2 (top right), the average of samples from anoxic conditions n=3 (bottom right). Pho-P = phosphonates, Di-P = diester-P, Mon-P = monoester-P. Polyphosphate was not detected at concentrations >1% in any of the samples analyzed. B) Average extracellular enzyme activities under oxic and anoxic conditions for MUP, DiMUP, PYRO-P and MUGb (n=5)